

University of Wollongong - Research Online

Thesis Collection

Title: Analysis of metal vapour generation by laser ablation

Author: Shervin Farjad

Year: 2007

Repository DOI:

Copyright Warning

You may print or download ONE copy of this document for the purpose of your own research or study. The University does not authorise you to copy, communicate or otherwise make available electronically to any other person any copyright material contained on this site.

You are reminded of the following: This work is copyright. Apart from any use permitted under the Copyright Act 1968, no part of this work may be reproduced by any process, nor may any other exclusive right be exercised, without the permission of the author. Copyright owners are entitled to take legal action against persons who infringe their copyright. A reproduction of material that is protected by copyright may be a copyright infringement. A court may impose penalties and award damages in relation to offences and infringements relating to copyright material.

Higher penalties may apply, and higher damages may be awarded, for offences and infringements involving the conversion of material into digital or electronic form.

Unless otherwise indicated, the views expressed in this thesis are those of the author and do not necessarily represent the views of the University of Wollongong.

Research Online is the open access repository for the University of Wollongong. For further information contact the UOW Library: research-pubs@uow.edu.au

University of Wollongong Thesis Collections

University of Wollongong Thesis Collection

University of Wollongong

Year 2007

Analysis of metal vapour generation by laser ablation

Shervin Farjad
University of Wollongong

Farjad, Shervin, Analysis of metal vapour generation by laser ablation, M.Eng. thesis, School of Mechanical, Material and Mechatronic Engineering, University of Wollongong, 2007.
<http://ro.uow.edu.au/theses/692>

This paper is posted at Research Online.
<http://ro.uow.edu.au/theses/692>

NOTE

This online version of the thesis may have different page formatting and pagination from the paper copy held in the University of Wollongong Library.

UNIVERSITY OF WOLLONGONG

COPYRIGHT WARNING

You may print or download ONE copy of this document for the purpose of your own research or study. The University does not authorise you to copy, communicate or otherwise make available electronically to any other person any copyright material contained on this site. You are reminded of the following:

Copyright owners are entitled to take legal action against persons who infringe their copyright. A reproduction of material that is protected by copyright may be a copyright infringement. A court may impose penalties and award damages in relation to offences and infringements relating to copyright material. Higher penalties may apply, and higher damages may be awarded, for offences and infringements involving the conversion of material into digital or electronic form.

ANALYSIS OF METAL VAPOUR GENERATION BY LASER ABLATION

A thesis submitted in (partial) fulfilment of the

requirements for the award of the degree

MASTER OF ENGINEERING (HONOURS)

from

UNIVERSITY OF WOLLONGONG

by

Shervin Farjad, B.E. (Hons)

School of Mechanical, Material and Mechatronic Engineering (MMM)

2007

CANDIDATE'S CERTIFICATE

I, Shervin Farjad, declare that this thesis, submitted in partial fulfilment of the requirements for the award of Master of Engineering - Research, in the Department of Mechanical, Materials and Mechatronic Engineering (MMM), University of Wollongong, is wholly my own work unless otherwise referenced or acknowledged. The document has not been submitted for qualifications at any other academic institution.

Shervin Farjad

28 / February / 2007

ACKNOWLEDGEMENTS

I wish to express my gratitude to my supervisor, Professor John Norrish for his patience and support during the formative stages of this thesis.

I wish to thank Joe Abbott for his collaboration during the experiments with LASER machine. Also, for their assistance during TEM and SEM experiments my thanks to Dr. Kristin Carpenter and Nick Mackie.

This is to acknowledge that the procedure of collecting fume on the TEM grid and particle analyses using *Scion* software are as Dr. Zoran Sterjovski, a researcher in University of Wollongong, developed through a project with BOC Australia.

I would like to thank my co-supervisor Dr. Brian Monaghan for his technical support during the absence of my supervisor.

I would be remiss without mentioning Dr. Mehrassa Farjad and Ehsan Keyhani whose cares made me feel at home.

Finally, I wish to dedicate this thesis to my parents, brothers and sister whom I owe what I have achieved.

ABSTRACT

A chamber for ablation purpose was designed. This system was calibrated and the minimum spot size produced by the LASER on the sample surface and its relation with sample position adjustment experimentally, was determined. Applying this chamber, a technique for controlled generation of particulate by LASER ablation has been developed. The sampling was carried out in four different atmospheres; Air, CO₂, Stainshield 66, and Argoshield 52. Furthermore, to survey and analyse the fume particle size range, *Scion Image* software was applied.

Scanning Electron Microscopy (SEM) and Transmission Electron Microscopy were chosen for analysis of fume particles morphology and size distribution. Energy Dispersive spectroscopy (EDS) and Scanning Transmission Electron Microscopy (STEM) were also chosen for chemical analysis.

The average fume particle size observed in all atmospheres was less than 0.1 micrometer. Considering the effect of oxidation potential of shielding gases, CO₂ generated the largest fume particles compared to Ar, while adding H₂ led to a smaller particles size.

The agglomeration pattern and morphology of fume particles was analysed as well. The survey of the agglomerated fume particles morphology with the SEM is more reliable since the TEM sample preparation could disturb the agglomeration pattern.

Fume particles agglomeration tended to grow three dimensionally while ferrous compound tended to make network and agglomerate together. The fume particles in the same size range tended to agglomerate in a 'chain' pattern which could grow up to 10 micrometers. The population of agglomerated particles with different sizes together varied between 3 and 400 particles. One of the most common patterns of these agglomerations is 'spherical' pattern.

While the fume particles can be in 'faceted' or 'spherical' shape, fume particles observed in this work were mainly 'faceted', independent of applied atmosphere.

The chemical composition of fume particles is variable of target (the sample) composition. In this work Fe, Mn, Si and O₂ were the elements observed in fume particles composition, while the elements found in the fume particles did not vary in different atmospheres.

It is also proposed that future works follow the investigation of the size distribution and morphology of fume particles while different welding electrodes are targeted by LASER and atmosphere is purged with shielding gases.

TABLE OF CONTENTS

	PAGE
ACKNOWLEDGEMENTS.....	II
ABSTRACT.....	III
TABLE OF CONTENTS.....	IV
1. INTRODUCTION.....	1
2. LITERATURE REVIEW.....	3
2-1. Why is the study of the fume important?	4
2-2. Welding fumes.....	4
2-2-1. Particulate fume.....	4
2-2-1-1. Aluminium.....	4
2-2-1-2. Cadmium.....	5
2-2-1-3. Chromium.....	5
2-2-1-4. Copper.....	6
2-2-1-5. Manganese.....	6
2-2-1-6. Nickel	7
2-2-1-7. Vanadium.....	7
2-2-1-8. Zinc	8
2-2-1-9. Fluorides	8
2-2-1-10. Iron	9
2-2-1-11. Lead	9
2-2-1-12. Silica	9
2-2-1-13. Other fumes.....	9
2-2-2. Gases.....	9
2-2-2-1. Carbon monoxide and Carbon dioxide	9
2-2-2-2. Ozone	10
2-2-2-3. Nitrogen dioxide.....	10
2-2-2-4. Chlorinated hydrocarbons and Phosgene	10
2-3. How do these gases threaten the human health?	11
2-3-1. Respiratory damages.....	12
2-3-1-1. Pulmonary Function.....	12
2-3-1-2. Asthma.....	12
2-3-1-3. Metal Fume Fever (MFF).....	13
2-3-1-4. Bronchitis.....	13
2-3-1-5. Pneumoconiosis and Fibrosis.....	13
2-3-1-6. Respiratory Infection and Immunity.....	14
2-3-1-7. Lung Cancer.....	15
2-3-2. Non-Respiratory damages	15
2-3-2-1. Dermatological and Hypersensitivity Effects.....	15
2-3-2-2. Central Nervous System Effects.....	15
2-3-2-3. Prostate Cancer	15

	PAGE
2-3-2-4. Reproductive Effects.....	15
2-4. Fumes and gases allowance.....	18
2-5. Recommended control methods.....	19
2-6. Fume formation mechanism.....	20
2-7. Parameters which affect the fume formation.....	20
2-8. LASER technology.....	21
2-9. LASER ablation and its Usages	21
2-10. Ablation Parameters.....	22
2-10-1. Sampling Strategy.....	22
2-10-2. Chamber Shape.....	22
2-10-3. Sample Roughness.....	22
2-10-4. Transport System and carrier gas.....	23
2-11. LASER in welding.....	23
2-12. Diode LASER	32
2-13. Shielding gases	32
2-14. Traditional fume sampling.....	33
2-15. Particle size and morphology.....	40
2-16. Factors that affect fume generation.....	44
2-16-1. Shielding gas.....	44
2-16-2. Base metal composition.....	45
2-17. Sample analysis.....	45
3. EXPERIMENTAL PROCEDURE.....	49
3-1. LASER ablation chamber design.....	50
3-1-1. Objectives.....	50
3-1-2. Chamber design.....	50
3-1-3. Prospective materials and dimensions.....	51
3-1-4. Safety issues.....	51
3-2. New chamber adaptation.....	51
3-3. Sampling method.....	57
3-4. LASER spot size output.....	57
3-5. Weighing experiments.....	58
3-6. Generating fume weight Vs. Focal length in different atmospheres.....	58
3-7. Generating fume weight Vs. Laser power in different atmospheres.....	60
3-8. Analyses.....	62
3-8-1. SEM.....	62
3-8-1-1. Sample preparation and Imaging.....	62
3-8-1-2. EDS analysis.....	64
3-8-2. TEM.....	65
3-8-2-1. Sample preparation.....	65
3-8-2-2. TEM Imaging.....	67

	PAGE
3-8-2-3. EDS and STEM analyses.....	68
3-8-2-4. Particle Size Analysis.....	69
4. EXPERIMENTAL RESULTS.....	70
4-1. LASER chamber characteristics.....	71
4-2. Weighing experiments.....	73
4-3. SEM.....	75
4-3-1. Images.....	75
4-3-2. EDS and Map of elements.....	77
4-4. TEM	79
4-4-1. Images.....	79
4-4-2. EDS and map of elements.....	82
4-4-3. Particle Size Analysis.....	84
5. DISCUSSION.....	87
5-1. Chamber characteristics.....	88
5-2. Weighing experiments.....	88
5-3. Fume particle size.....	89
5-4. Fume morphology.....	90
5-5. Fume particle compounds.....	90
5-6. Recommendation.....	91
6. CONCLUSIONS.....	92
REFERENCES.....	94
APPENDIX.....	99

CHAPTER ONE

INTRODUCTION

Fumes and gases generated during the welding processes may expose welders to the short term or even acute health consequences [1]. Although substantial researches have been conducted in order to analyse the fume particulates and the parameters which affect the fume formation and its characteristics, the discrepancies in results emphasize the importance of more accurate investigations.

Ablation is a method in which a surface is evaporated by usage a LASER [25]. In present work this ablation process was used to generate fume under controlled condition and more particularly, controlled atmosphere. Stainshield 66, Argoshield 52, CO₂ and Air are the atmospheres in which ablation was conducted.

The application of a LASER for fume generation by ablation is a novel idea therefore, establishing the characteristics of the ablation device, set up the sampling method, examining the repeatability of experiments and finding the appropriate analyses were the priorities of this work. These procedures are explained in chapter three.

Scanning Electron Microscopy (SEM) and Transmission Electron Microscopy were chosen for analysis of the fume particles morphology and size distribution. Also, Energy Dispersive spectroscopy (EDS) and Scanning Transmission Electron Microscopy (STEM) are the methods which were chosen for chemical analysis. Moreover, the *Scion Image* software was applied to survey and analyse the fume particle size range. Furthermore, the chemical composition, morphology and size distribution were investigated during the fume particle analysis of this thesis.

While chapter four conveys the results of experiments, chapter five discusses the results against the literature. This thesis is concluded in chapter six which followed by the recommendations for future researches.

CHAPTER TWO

LITERATURE REVIEW

2-1 Why is the study of the fume important?

Fumes and gases generated during the welding process may expose welders to the short term or even acute health consequences. Metal fume fever (MFF), drowsiness, sore eyes, throat and lung irritation are the examples of short term effects [1]. However, the substantial concern has recently expressed related to possible long-term effects such as cancers, respiratory and cardiovascular diseases and neurodegenerative diseases [1, 2].

Up to two percents of workers in different industries around the world are believed to be involved in welding processes [16], and the population who potentially are at risk is significant [3]. Despite some controls are implemented to reduce exposure, welders may still be exposed to hazardous fumes [4]. Researchers in the medical field are trying to determine the effect of some constituent in human body and related diseases and problems. Similarly, in engineering field researchers are trying to find out the parameters influencing on fume generation.

Although the substantial investigations regarding to the fume sampling and analysis have been undertaken, the parameters controlling the fume generation process have yet to be determined. In this thesis a method of sampling and analysing fume by the means of Diode-LASER ablation is investigated in an attempt to clarify fume generation effect.

2-2 Welding fumes

Welding fume consists of two components; particulate welding fumes and gases [16].

2-2-1 Particulate Fume

The base metal, welding consumable, and surface coating in the vicinity of welding zone are vaporized [3]. The vapour is then condensed to the solid particles and as a result of high temperature and exposure to Oxygen may become oxidized [16].

Some of the more common constituents of welding fume are considered below:

2-2-1-1 Aluminium

The normal level of Aluminium in the environment is shown in table 2-1. The amount of Aluminium daily exposure from this ambient level is negligible but much higher levels are generated during the welding [5].

Aluminium commonly is used in ferrous and non-ferrous material as an additive as well as electroplated layers, hot dip coatings, paints, filler wires and electrodes [16].

The welding of Aluminium is also associated with in Ozone and pneumotoxic gas generation [16].

Table 2-1: The ambient level of AL [5].

	Background ^a	Rural ^a	Urban ^a
Average air level*	0.005-0.018 ^b	0.27-0.38 ^c 0.005-0.0032 ^d	0.4-10.0 ^b

* *Nanograms Aluminium per cubic meter*

a [6]

b United States

c Central Canada

d Rural Hawaii

2-2-1-2 Cadmium

The amount of Cd in environment is shown in table 2- 2. Owing to volatile nature of Cd, the existence of this element in the base metal, or any substances near the welding zone is potentially hazardous [5].

Cadmium usually is used on the steels as a coating in order to prevent rusting [3]. Also, it is widely used in FCAW as an ingredient of flux [16].

Table 2-2: The ambient level of Cd [5].

	Background ^a	Rural ^a	Urban ^a
Average air level*	<1 ^b	<4-4.5 ^c	3-40 ^b <4-10 ^d <4-115 ^e

* *Nanograms of Cd per cubic meter*

a [8]

b United States

c Rural Illinois

d Chicago

e East St. Louis

2-2-1-3 Chromium

Chromium is the element which may exist as a pollutant in air as shown in table 2-3. It tends to exist higher than average in the United States [5]. In industry, Chromium is significantly used in Stainless Steels, Cast Irons, Paints, dye, corrosion inhibitors and pigments [5].

Table 2-3: The ambient level of Cr [5].

	Background^a	Rural^a	Urban^a
Average air level*	0.005-2.6 ^b	<10 ^b	10-30 ^b >500 ^c >225 ^d 100-400 ^e

* Nanograms of Cr per cubic meter

a [9]

b United States

c Steubenville, OH.

d Baltimore, MD.

e Corpus Christi, TX.

2-2-1-4 Copper

The concentration of Copper in breathing zone is directly related to proximately to the source of generation [5]. The level of Copper in the environment is shows in table 2-4.

Copper is used in order to prevent rusting [3]. In particular, the existence of Copper in breathing zone will be aggravated when the Copper welding is practiced [16].

Table 2-4: The ambient level of Cu [5].

	Background^a	Rural^a	Urban^a
Average air level*	0.029-12 ^{b, f}	5-50 ^{b, e} 3-280 ^{b, f}	20-200 ^{b, e} 3-5100 ^{b, f} 17-500 ^c 13-2750 ^d

* Nanograms of Cu per cubic meter

a [10]

b United States

c Canada

d Europe

e Davies and Bennet, 1985

f Schroeder et al., 1987

2-2-1-5 Manganese

The existence of Manganese in breathing zone is directly related to the generation source proximity [5].

The level of Mn in environment is shown in table 2-5.

Manganese is commonly used in steel, in Flux-Cored Arc electrodes and as a flux in coating of Shielded Metal Arc electrodes [16].

Table 2-5: The ambient level of Mn [5].

	Background ^a	Rural ^a	Urban ^a
Average air level*	1-3 ^b	5-60 ^{b, c}	33-110 ^{b, c} 130-150 ^{b, d}

* *Nanograms of Mn per cubic meter*

a [11]

b United States

c Low-end values shown are those from most recent studies, indicative of a downward trend over the past 50 years

d Source-dominated site values

2-2-1-6 Nickel

Nickel can be found in several different valencies in the atmosphere but most toxic form of those is Ni²⁺ [5].

Table 2-6 shows the level of Ni in environment.

Nickel can be found in the breathing zone during Stainless Steels welding [16].

Table 2-6: The ambient level of Ni [5].

	Background ^a	Rural ^a	Urban ^a
Average air level*	0.14-0.45 ^{a, d}	0.6-78 ^{a, b} 6-17 ^{b, c} ~1.0 ^{a, d}	1-328 ^{a, b} 120-170 ^{b, c} 1-20 ^{a, d}

* *Nanograms of Ni per cubic meter*

a [12]

b United States

c Costa, 2000

d Canada, many state

2-2-1-7 Vanadium

Vanadium can commonly be found in atmosphere as is shown in table 2-7 [5].

Table 2-7: The ambient level of V [5].

	Background ^a	Rural ^a	Urban ^a
Average air level*	0.001-0.002 ^a	1-40 ^b 0.21-1.9 ^c 0.02-0.80 ^d	3-22 ^b 150-1400 ^e

* Nanograms of V per cubic meter

a [13]

b United States

c Northwest Canada

d Eastern Pacific

e North-eastern United States

2-2-1-8 Zinc

Zinc is one of the most common metals can be found in air [5].Table 2-8 shows the level of this element in environment.

The level of Zinc in welding environment is increased when galvanized or Zinc coated steel are being welded [16].

Table 2-8: The Ambient level of Zn [5].

	Background ^a	Rural ^a	Urban ^a
Average air level*	3-27 ^b	10-50 ^b 20-160 ^e 20-60 ^f	293-380 ^c 27-500 ^d 20-160 ^b 170-670 ^e 70-590 ^f

* Nanograms of Zn per cubic meter

a [15]

b United States

c New York City

d San Francisco Bay area

e Seven U.S. cities/2 rural sites

f New Jersey

2-2-1-9 Fluorides

Fluorides are originated from cover of Metal Arc electrodes, flux or slag of Flux-Cored Arc electrodes and Self-shielded Flux-Cored electrodes which contains Fluorspar [16].

2-2-1-10 Iron

The principal vapour formed in steel welding fume is Iron oxide which originates from base metal and the electrode [3, 16].

2-2-1-11 Lead

During the welding or cutting of the Lead bearing alloys Lead oxides may be generated [3].

2-2-1-12 Silica

The coating of Manual Metal electrodes and the flux of Flux-Cored electrodes is the main sources of Silica during the welding [16].

Silica could be generated from Ferro silicate, kaolin, Feldspar, Mica, Talc, or Waterglass existing in flux composition [16].

2-2-1-13 Other fumes

Magnesium, Molybdenum, Titanium, Barium, Beryllium, Calcium oxide, Cobalt, Lithium, Phosphorous, Platinum, Selenium, Silver, Sodium, Tellurium, Yttrium and Zirconium may also be present in fumes which are generated during the welding procedure [3].

2-2-2 Gases

The amount and type of gases generated during the welding process depend on:

- Shielding gases
- Composition of electrode coating and core
- Reaction in the arc with atmospheric constituents
- Reaction of ultraviolet light with atmospheric gases
- Composition of cleaning material
- Composition of any coating layer on the metal

Ozone, Nitrogen oxides, Carbon monoxide, and Carbon dioxide are the main gases formed during welding processes [16].

2-2-2-1 Carbon monoxide and Carbon dioxide

Carbon monoxide is odourless, colourless and tasteless gas which usually is produced during the incomplete fuel combustion [3].

Inorganic carbonate (like CaCO_3 ; Lime) and Organic compounds of electrodes coatings and cores, and shielding gases (CO_2 or argon/ CO_2 mixtures) are the sources of Carbon dioxide and Carbon monoxide [16].

Since Carbon monoxide is chemically more stable than Carbon dioxide at high temperature, Carbon dioxide will change to Carbon monoxide in arc [16].

2-2-2-2 Ozone

As a result of photochemical reaction activated by Ultra Violet (UV) radiation from the arc welding Ozone may be formed [16].



The amount of produced Ozone depends on the amount and wavelength of Ultra Violet radiation in the welding area. The intensity and wavelength of UV itself is influenced by welding variables such as voltage, current, shielding gas, type of electrode, arc length and type of welding [16]. For instance GMAW, GTAW and Plasma arc cutting produce high intensity UV and accordingly high amounts of Ozone [3].

2-2-2-3 Nitrogen dioxide

When the atmospheric Nitrogen at high welding temperature reacts with Oxygen, forms Nitrogen monoxide;



Above 1200° C the reaction rate will increase and consequently the Nitrogen monoxide will react with Oxygen to form Nitrogen dioxide [16].



As with Ozone, GMAW, GTAW and Plasma arc welding are known as a processes which generate a large amount of NO₂ the existence of Nitrogen in shielding gas will increase the generated amount of NO₂ [3].

2-2-2-4 Chlorinated hydrocarbons and Phosgene

Chlorinated hydrocarbons are used for degreasing and cleaning and as a result of decomposition in the welding arc produce Phosgene gas [3].

Trichloroethylene is a common chlorinated hydrocarbon often used for cleaning [16]. It has a high vapour pressure [16]. As a result of existence of Oxygen, Trichloroethylene and Ultra Violet radiation in welding area the Phosgene is generated [16].

2-3 How do these gases threaten the human health?

The recent epidemiological studies regarding short time and long term effects of welding fumes exposure indicate the incidence of Respiratory Irritation, Bronchitis, Pneumoconiosis, Parkinsonism, Lung Cancer and Pulmonary Infections among the welders [2, 16, 17].

These epidemiological studies have been undertaken in a range of [16]:

- Industrial settings
- Worker populations
- Duration of exposure
- Welding techniques
- Occupational exposures
- Carefully controlled work environments
- Actual workplace conditions

Researchers in the field of Immunotoxicology as well as Pulmonary Toxicology have been targeting the effect of toxic fume on respiratory and immune system of welders [5]. They have undertaken underlying research on the laboratory rats and human models both in actual and laboratory working environment [16, 5].

Antonini reviews the health disorders caused by fumes and gases in the following groups [16]:

➤ Respiratory

- Pulmonary Function
- Asthma
- Metal Fume Fever(MFF)
- Bronchitis
- Pneumoconiosis and Fibrosis
- Respiratory Infection and Immunity
- Lung Cancer

➤ Non-Respiratory

- Dermatological and Hypersensitivity Effects
- Central Nervous System Effects
- Prostate Cancer [19]
- Reproductive Effects

2-3-1 Respiratory damages

2-3-1-1 Pulmonary Function

Some researchers argue that Fibrosis and Emphysema, which reduce the pulmonary expansion and elasticity are not strictly originated from welding fumes and mainly other factors like smoking, life style, genetic history, obesity, and etc. are responsible [16, 18,19]. However, some cases indicate that the working in confined area, frequently exposure and inhaling the high level of welding fume even in non-smoker welders cause serious pulmonary problems [17].

The following fumes and gases are known to lead to pulmonary malfunction [3]:

- Cadmium in Emphysema and pulmonary dema
- Beryllium in Pneumonia
- Copper in Respiratory failure
- Fluoride in pulmonary dema
- Ozone in dryness of upper respiratory tracts

Sjogren (2004) shows that the Fluoride has the strongest effect on respiratory malfunction [22]. Table 2-9 shows the Urinary Fluoride concentration and related respiratory symptom among welders [22].

Table 2-9: The Urinary Fluoride concentration and respiratory symptom among welders [22].

	0.2-0.4 mg/L		0.5-0.9 mg/L		1.0-3.0 mg/L	
	With symptoms	Total No.	With symptoms	Total No.	With symptoms	Total No.
All	2	18	6	19	9	26
Non-smokers	2	10	2	11	5	16
Smokers	0	8	4	8	4	10

2-3-1-2 Asthma

The specific sensitizing compounds in the working place result in occupational Asthma [16]. This kind of Asthma clearly is different from Nonoccupational Asthma [16].

Howden suggests that Nickel and Chromium in welding of Stainless steel are examples of these sensitizing Asthma agents [16].

Wang, et al., Meredith, Beach, et al., Simonsson, et al., Palmer and Eaton reported the relation between welding fume and Asthma [16]. Nitrogen Oxide, Ozone, Beryllium are also considered as sensitizing agents which cause Asthma and 'Breath shortening' [3].

2-3-1-3 Metal Fume Fever (MFF)

The most common fume exposure illness which has been observed is Metal Fume Fever (MFF) [16].

Although Borak, Cohen and Hethmon argue that Copper and Zinc are the agents which can cause the acute febrile illness and Pneumonitis rather than the MFF [15]. Sterilize & Beckett suggest that Zinc is the responsible of MFF particularly during the welding of galvanized steel or alloys coated or containing Zinc [16].

Liss argues that Cadmium, Magnesium and Copper fume inhalation will lead to MFF [16]. Liss continues that the symptoms of MFF are:

- Thirst
- Dry cough
- Sweet or metallic taste in the
- Mouth
- Chills
- Dyspnea
- Malaise
- Muscle aches
- Headaches
- Nausea

These can often be felt in some hours after welding is carried out [16]. However, the etiology of MFF has not been clearly defined [16].

2-3-1-4 Bronchitis

Inflammation in the respiratory tract is known as Bronchitis and can be identified from coughing or mucus expectation [16]. Villaume, et al. indicate that Nitrogen dioxide and Sulphur dioxide are the main agents responsible for Bronchitis [19].

While some studies show that Bronchitis is only observed in smoker welders, some cases report that lifetime no-smoker welders exhibit Bronchitis and respiratory inflammation [16, 17].

Mur claims that smoking and exposure to welding fume extensively increase the threat of Bronchitis in welders. Mur continues that the occurrence of Bronchitis in MMAW is more than GMAW [20].

Beckett, et al. launched a survey of shipyard welders over 3 years. Beckett, et al. show the incidence of cough, Phlegm, wheezing, and chest tightness in 35% of welder during the workdays which improved at weekends [21].

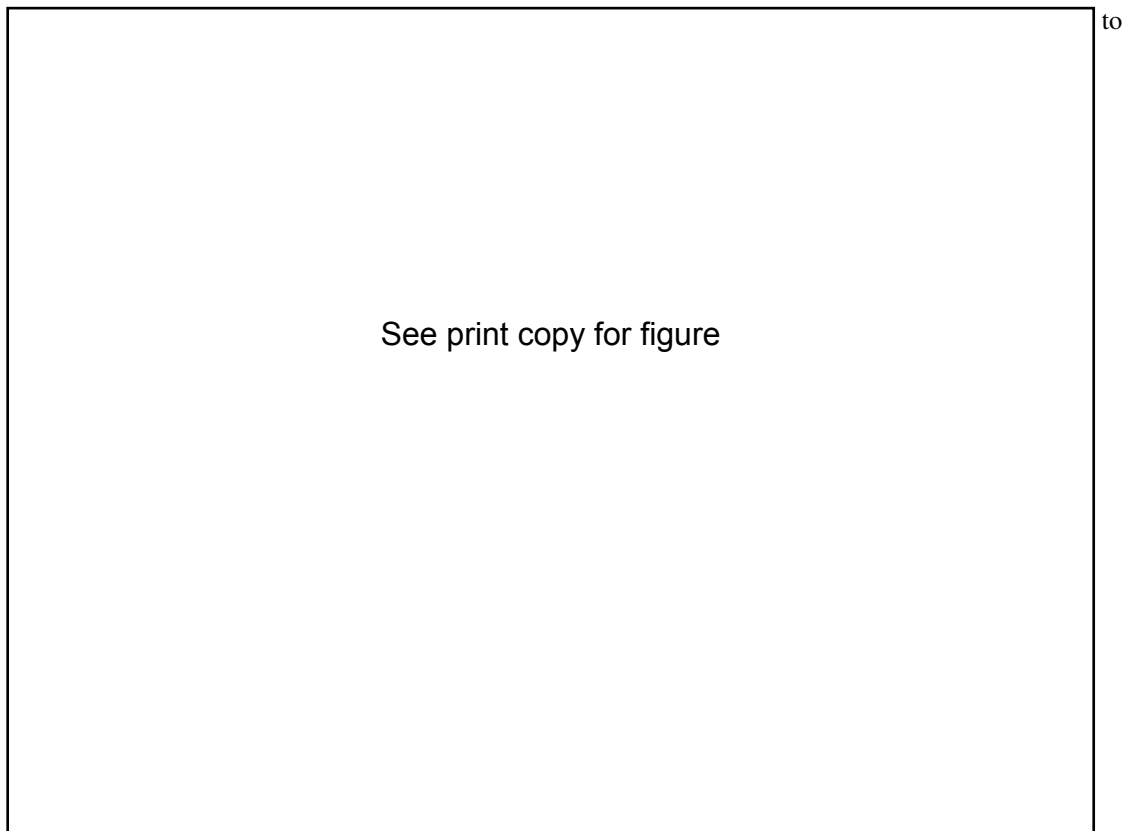
2-3-1-5 Pneumoconiosis and Fibrosis

Siderosis is a condition associates with exposure to a high amount of Iron oxide and was observed in biopsy of lung without any symptom of Pneumoconiosis [16]. While in most reported cases Siderosis was observed

in welders, Funahashi, et al. (1988) show that alveolar wall thickening and some degree of Fibrosis can be observed in all welders [16].

Silica, Iron, Aluminium and Carbon contained fumes have been known that can result the Siderosis, Fibrosis and Pneumoconiosis [16, 17].

Some researches have investigated in relation to the effect of age, height and physics of welders on these lung abnormalities. Roesler & Weitowiltz (1996) argue that duration of exposure and working in confined area is the most important agent which leads to Pneumoconiosis and Fibrosis [16]. Ron Balkissoon reports a 26 years old non-smoker welder whose lung biopsy shows the Aluminium Pneumoconiosis [17]. Figure 2-1 shows the biopsy sample of his lung with the inflammation Aluminium Pneumoconiosis.



2-3-1-6 Respiratory Infection and Immunity

Howden, et al. (1998) argue that frequency, duration and severity of exposure increase the probability of acute upper or lower respiratory tract [16]. Doig & Challen (1964) suggest that Pneumonia in welders is related to working duration not the age of welders [16].

Beaumont (1980) claims that Nitrogen dioxide and Ozone are the agents which cause Pneumonia and may have a fatal effect on welders [16].

2-3-1-7 Lung Cancer

Researches about the effect of welding fumes and gases on lung cancer do not show certainty [16]. However, Hedenstedt, et al. (1977), Maxild, et al. (1978) and Stern, et al. (1988) contend that Chromium and Nickel existing in welding fumes are carcinogenic [16]. Danielson, et al. (2000) after examining 860 shipyard welders indicates that the relative risk of cancer is 1.90 [16].

It has been shown that Cadmium inhalation possibly can cause lung cancer [19].

2-3-2 Non-Respiratory damages

2-3-2-1 Dermatological and Hypersensitivity Effects

Skin sensitizing or irritation can be generated by contact with Chromium, Nickel, Zinc, Cobalt, Cadmium, Molybdenum, and Tungsten. Fregert & Ovrup (1963) report Chromate sensitization and allergic dermatitis among steel welders [16].

Weiler (1979) reports that Nickel can cause Eczema [16].

2-3-2-2 Central Nervous System Effects

Lead, Aluminium and most specifically Manganese are known that contribute to Psychiatric symptoms [16]. Lucchini, et al. (1999) indicate that exposure to low amounts of Manganese for a long time may end in neuro functional disorders in welders. Anatovskaia (1984) claims that weakness, exhaustion, fatigue, apathy, dizziness, imbalance, numbness, irritability, memory loss and Parkinson are the other effects of Manganese Oxide inhalation [2, 16, 23].

2-3-2-3 Prostate Cancer

The International Agency for Research on Cancer in 1993 categorised Cadmium and its compounds as carcinogenic “group 1”. While the research results show uncertainty about Cadmium effects as well as smoking habits, Nickel hydroxide and Lead on Prostate cancer [19].

2-3-2-4 Reproductive Effects

Chromium, Cadmium, Lead and Manganese compounds are reported as agents which negatively affect male fertility [16]. Mortensen (1988) shows that the risk of fertility abnormality for Stainless Steel welders is 2.34 times by comparison to normal people [16]. Table 2-10 shows a review on fumes and gases generating during the welding and allied processes and their effects on human health [22].

Table 2-10: A review on fumes and gases generating during the welding and allied processes and their effects on human health [22].

	Source	Effects and Symptoms
FUMES		
Aluminum	Aluminum component of some alloys, e.g., Inconels, copper, zinc, steel, magnesium, brass and filler materials.	Respiratory irritant.
Beryllium	Hardening agent found in copper, magnesium, aluminum alloys and electrical contacts.	"Metal Fume Fever." A carcinogen. Other chronic effects include damage to the respiratory tract.
Cadmium Oxides	Stainless steel containing cadmium or plated materials, zinc alloy.	Irritation of respiratory system, sore and dry throat, chest pain and breathing difficulty. Chronic effects include kidney damage and emphysema. Suspected carcinogen.
Chromium	Most stainless-steel and high-alloy materials, welding rods. Also used as plating material.	Increased risk of lung cancer. Some individuals may develop skin irritation. Some forms are carcinogens (hexavalent chromium).
Copper	Alloys such as Monel, brass, bronze. Also some welding rods.	Acute effects include irritation of the eyes, nose and throat, nausea and "Metal Fume Fever."
Fluorides	Common electrode coating and flux material for both low- and high-alloy steels.	Acute effect is irritation of the eyes, nose and throat. Long-term exposures may result in bone and joint problems. Chronic effects also include excess fluid in the lungs.
Iron Oxide	The major component in all iron or steel welding processes.	Siderosis – a benign form of lung disease caused by particles deposited in the lungs. Acute symptoms include irritation of the nose and lungs. Tends to clear up when exposure stops.
Lead	Solder, brass and bronze alloys, primer/coating on steels.	Chronic effects to nervous system, kidneys, digestive system and mental capacity. Can cause lead poisoning.

	Source	Effects and Symptoms
Manganese	Most welding processes, especially high-tensile steels.	"Metal Fume Fever." Chronic effects may include central nervous system problems.
Molybdenum	Steel alloys, iron, stainless steel, nickel alloys.	Acute effects are eye, nose and throat irritation, and shortness of breath.
Nickel	Stainless steel, Inconel, Monel, Hastelloy and other high-alloy materials, welding rods and plated steel.	Acute effect is irritation of the eyes, nose and throat. Increased cancer risk has been noted in occupations other than welding. Also associated with dermatitis and lung problems.
Vanadium	Some steel alloys, iron, stainless steel, nickel alloys.	Acute effect is irritation of the eyes, skin and respiratory tract. Chronic effects include bronchitis, retinitis, fluid in the lungs and pneumonia.
Zinc Oxides	Galvanized and painted metal.	"Metal Fume Fever."
GASES		
Carbon Monoxide	Formed in the arc.	Absorbed readily into the bloodstream, causing headaches, dizziness or muscular weakness. High concentrations may result in unconsciousness and death.
Hydrogen Fluoride	Decomposition of rod coatings.	Irritating to the eyes and respiratory tract. Overexposure can cause lung, kidney, bone and liver damage. Chronic exposure can result in chronic irritation of the nose, throat and bronchi.
Nitrogen Oxide	Formed in the arc.	Eye, nose and throat irritation in low concentrations. Abnormal fluid in the lung and other serious effects at higher concentrations. Chronic effects include lung problems such as emphysema.
Oxygen Deficiency	Welding in confined spaces, and air displacement by shielding gas.	Dizziness, mental confusion, asphyxiation and death.
Ozone	Formed in the welding arc, especially during plasma-arc, MIG and TIG processes.	Acute effects include fluid in the lungs and hemorrhaging. Very low concentrations (e.g., one part per million) cause headaches and dryness of the eyes. Chronic effects include significant changes in lung function.

	Source	Effects and Symptoms
ORGANIC VAPOURS		
Aldehydes (such as formaldehyde)	Metal coating with binders and pigments. Degreasing solvents.	Irritant to eyes and respiratory tract.
Di-isocyanates	Metal with polyurethane paint.	Eye, nose and throat irritation. High possibility of sensitization, producing asthmatic or other allergic symptoms, even at very low exposures.
Phosgene	Metal with residual degreasing solvents. (Phosgene is formed by reaction of the solvent and welding radiation.)	Severe irritant to eyes, nose and respiratory system. Symptoms may be delayed.
Phosphine	Metal coated with rust inhibitors. (Phosphine is formed by reaction of the rust inhibitor with welding radiation.)	Irritant to eyes and respiratory system, can damage kidneys and other organs.

2-4 Fumes and gases allowance

In order to provide safe working limits for workers exposed to fumes and gases a range of values have been published.

Exposure limits of fumes and gases may be sourced from different international organisation such as:

- The U.S. Department of Labour (OSHA) Permissible Exposure Limits (PELs)
- NIOSH Recommended Exposure Limits (RELs)
- The American Conference of Governmental Industrial Hygienist's (ACGIH) Threshold Limit Values (TLVs) [4]

In 1989 the PEL for total fumes was considered at 5 mg/m^3 , $5000 \text{ }\mu\text{g/m}^3$, in 8-hour Time-Weighted Average (TWA) and PEL for total Particulate Not Otherwise Regulated (PNOR) at 15 mg/m^3 in 8-hour time-weighted average (TWA) [4].

Considering the possible interaction between welding fumes and gases NIOSH suggested that the exposure limits should be set for each gas and fume (as shown in table 2-11) [4].

Verma (2000) contends that these exposure limits should be revised for unusual working schedule and shifts. Verma recommends that the equivalent PEL should be calculated according to biological half life of each element and working schedule [23].

Table 2-11: A summary of different substances exposure limits [4].

Substance	OSHA PEL-TWA ($\mu\text{g}/\text{m}^3$)	NIOSH REL-TWA ($\mu\text{g}/\text{m}^3$)	ACGIH TLV-TWA ($\mu\text{g}/\text{m}^3$)
Aluminum Fume	15,000 (Total) 5,000 (Respirable)	5,000	5,000
Arsenic	10	2 (Ceiling)	10
Barium	500	500	500
Beryllium	2	0.5 (Ceiling)	2
Calcium Oxide	--	2,000	2,000
Cadmium Fume	5	LFC (Ca)	10 (Total) 2 (Respirable)
Cobalt	100	50	20
Chromium, Hexavalent	--	1	50
Chromium, Metal	1,000	500	500
Copper Fume	100	100	200
Iron Oxide Fume	10,000 (as Fe)	5,000	5,000
Lithium	--	--	--
Magnesium Oxide	15,000	--	10,000
Manganese	5,000 (Ceiling)	1,000	200
Molybdenum	5,000 (Soluble) 15,000 (Insoluble)	--	5,000 (Soluble) 10,000 (Insoluble)
Nickel	1,000	15 (Ca)	1,000
Lead	50	100	50
Phosphorus	100	100	100
Platinum	2 (Soluble)	1,000 (Metal) 2 (Soluble)	1,000
Selenium	200	200	200
Silver	10	10	100
Sodium	--	--	--
Tellurium	100	100	100
Thallium	100	100 (Soluble)	100
Titanium Dioxide	15,000	LFC (Ca)	10,000
Vanadium Pentoxide	100 (Ceiling)	50 (Ceiling)	50
Yttrium	1,000	1,000	1,000
Zinc Oxide Fume	5,000	5,000	5,000
Zirconium	5,000	5,000	5,000
Welding Fumes	--	LFC (Ca)	5,000

LFC=lowest feasible concentration

Ca=NIOSH potential occupational carcinogen

2-5 Recommended control methods

For welding processes a number of controls have been suggested according to standard ANSI Z49.1, “Safety in welding and cutting”. These safety measures can be summarised as [3]:

- Process enclosure

- Local exhaust ventilation
- General dilution ventilation

2-6 Fume formation mechanism

Heile & Hill (1975) explain the fume formation mechanism as below order [39]:

- Vaporization of the elements
- Condensation
- Oxidization

Kobayashi, Maki, Hashimoto, and Suga (1978) by using a high speed camera show that welding fume is generated by vaporization of molten material, oxidization during their contact with air and condensation [39].

2-7 Parameters which affect the fume formation

Corderoy, Wills, and Wallwork (1980) show that the composition of shielding gas affects the composition of generated fumes [39].

Gray, Hewitt, and Hicks (1980) reported that the Oxygen potential of shielding gas affects on Fume Formation Rate. They reported that by increasing the Oxygen in shielding gas the FFR will increase [39].

Heile & Hill (1975) found that the fume formation rate (FFR) in GTAW, SMAW, GMAW deepens on voltage, current, welding travel speed and plate thickness [39]. Mendez, Jenkins, and Eager assert that the most important factor on generated fume amount is the temperature of welding area [40]. Their experiment was based on GMAW process which shows that increasing the temperature of welding area leads in higher evaporation [40].

Pires, Quintino, and Miranda surveyed the effect of shielding gas and current on fume formation rate in GMAW process [41]. Table 2-12 shows the effect of shielding gas mixture on Fume Formation Rate (FFR) [41]. Figure 2-2 shows the effect of gas Mixture and Current on Fume Formation Rate (FFR) [41]. In present work LASER is used for ablation in order to separate the effect of arc on fume formation mechanism.

Table 2-12: The effect of shielding gas mixture on Fume Formation Rate (FFR) [41].

Gas mixtures	Minimum FFR (g/min)	Maximum FFR (g/min)
Ar + 2%CO ₂	0.02	0.17
Ar + 8%CO ₂	0.05	0.22
Ar + 18%CO ₂	0.06	0.28
Ar + 5%O ₂	0.03	0.19
Ar + 8%O ₂	0.04	0.21
Ar + 3%CO ₂ + 1%O ₂	0.02	0.18
Ar + 5%CO ₂ + 4%O ₂	0.04	0.26

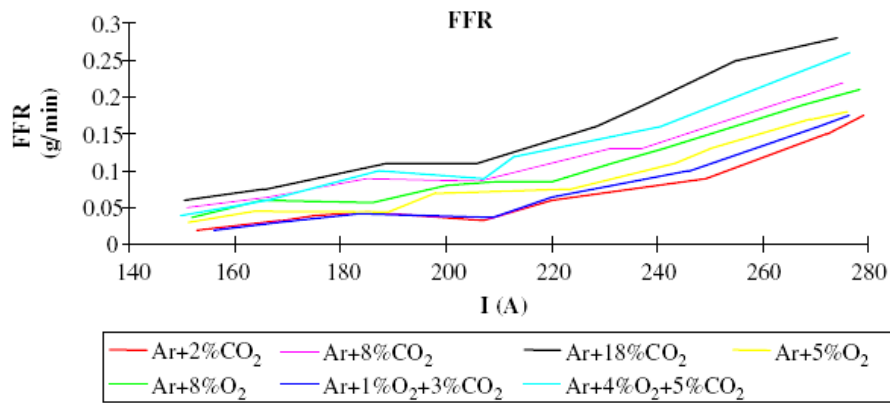


Figure 2-2: The effect of gas Mixture and Current on Fume Formation Rate (FFR) [41].

2-8 LASER technology

Light Amplification by Stimulated Emission of Radiation (LASER) was developed in the period 1950 to 1960 [24]. LASER devices produce Coherent, Monochromatic and intense radiation (1mW-100MW) and cover the wavelength from the Ultra violet to Infrared (600-1600 nm) [24]. In order to emit a photon of light, a atom or molecule of source should be excited to a state, in which the electron in ground state absorbs specific energy equal to ΔE^* (Equation 2-5) and goes to the higher energy state [24]. A LASER simulated emission occurs when the excited electron interacts with another photon and both emit in same phase (coherency). Similar, when these two electrons interact with two other electron then four, then eight and so on, a coherent "Cascade of emerging photons" is emitted [24].

Normally, the time period of excitation and decay of electrons is about picosecond to nanosecond which is not enough for simulation and producing the LASER (Lasing). Therefore, the excited electron is brought to other state with longer life long rather than ground state. This process is viable with changing the spin of excited electron (Inversion) [24].

The inversion process provide enough time for simulation. If this time is shorter than emission of light, a Pulse mode beam would be produced otherwise it would be in continuous mode [24].

$$\Delta E^* = h\nu = hc / \lambda \quad (2-5)$$

h: Planck's constant 6.63×10^{-23} J.sec

c: Velocity of light 3×10^8 m.sec⁻¹

ΔE^* : energy related to absorbed or emitted photon with given wavelength λ

2-9 LASER ablation and its Usages

Ablation is a process in which a surface is evaporated by usage a LASER [25]. In present work this ablation process is used to generate fume under controlled condition.

Geology, Earth science, and Medical science are the fields in which the LASER ablation has been employed [25]. Mason (2000) indicates that the Using the LASER ablation coupled with the Mass spectrometer, ICP-MS, is a strong devise for identifying elements like Silicate, Carbonate, Oxides and Sulphides [25]. Mason (2000) continues that in this process 100nm to 1µm from the surface of material is ablated and carrier gas such as Argon carries the vapour for the spectrometry analysis [25].

Using the Laser ablation to generate welding fumes is a noble application which is explored in this thesis.

2-10 Ablation Parameters

In recent researches regarding to identifying the elements in earth and medical sciences some parameters have been considered which are expected to lead to good results [25].

Mason (2000) suggests that the important parameters which can affect the result of ablation are [25]:

- Sampling Strategy
- Chamber Shape
- Sample Roughness
- Transport System and carrier gas

2-10-1 Sampling Strategy

There are two different methods of sampling; first, applying several consecutive pulses to single spot and second, the technique which is called “Raster”. In this technique the material is moved after each pulse to increase the sampling area [25].

2-10-2 Chamber Shape

Maschado & Simonelti (2000) argue that different kinds of Laser and spectrometer need different designs of chamber even though no single decision about the effectiveness of cells has been provided so far [25].

2-10-3 Sample Roughness

Maschado & Simonelti (2000) contend that the reduction in the surface roughness of material, improves the accuracy of the ablation results [25].

2-10-4 Transport System and carrier gas

Gunther (2000) suggests that carrier gas and transport system should not “dilute” the fumes [25].

Mason (2000) indicates the most important criteria in selecting the gas is the Ionisation potential of gases (see 2-16) [25].

2-11 LASER in welding

Several different types of LASERs have been used for manufacturing purposes. This application depends on the LASER wavelength, power, and type of the beam. Table 2-13 shows the different types of LASERs, and their characteristics and applications [26].

Table 2-13: Different types of LASERs, and their characteristics [26].

GAS LASER

LASER gain medium and type	Operation wavelength(s)	Pump source	Applications and notes
Helium-neon gas LASER	632.8nm (543.5nm, 593.9nm, 611.8nm, 1.1523µm, 1.52µm, 3.3913µm)	Electrical discharge	Interferometry, holography, spectroscopy, barcode scanning, alignment, optical demonstrations.
Argon ion gas LASER	488.0nm, 514.5nm, (351 nm, 465.8nm, 472.7nm, 528.7nm)	Electrical discharge	Retinal phototherapy (for diabetes), lithography, pumping other LASERs.
Krypton ion gas LASER	416nm, 530.9nm, 568.2 nm, 647.1nm, 676.4nm, 752.5nm, 799.3nm	Electrical discharge	Scientific research, mixed with Argon for creation of "white-light" LASERs, light shows.
Xenon ion gas LASER	Many lines throughout entire visible spectrum extending into the UV. and IR.	Electrical discharge	Scientific research.

LASER gain medium and type	Operation wavelength(s)	Pump source	Applications and notes
Nitrogen gas LASER	337.1nm	Electrical discharge	Pumping of dye LASERs, measurement of air pollution, scientific research, Nitrogen LASERs are capable of operating super radiantly (without a resonator cavity), and amateur LASER construction.
Hydrogen fluoride chemical LASER	2.7 to 2.9μm for (Hydrogen fluoride) 3.6 to 4.2μm for (Deuterium fluoride)	Chemical reaction in a burning jet of Ethylene and Nitrogen Trifluoride (NF ₃)	Used in research for LASER weaponry by the U.S. DOD, operated in continuous wave mode and capable of extremely high powers in the megawatt range.
Deuterium fluoride LASER	3800nm	Chemical reaction	
Chemical Oxygen-Iodine LASER (COIL)	1.315μm	Chemical reaction in a jet of singlet delta Oxygen and iodine	LASER weaponry, scientific and materials research, LASER used in the U.S. military's airborne LASER, operated in continuous wave mode and capable of extremely high powers in the megawatt range.
Carbon dioxide (CO ₂) gas LASER	10.6μm, (9.4μm)	Transverse (high power) or longitudinal (low power) electrical discharge	Material processing (cutting, welding, etc.), surgery.
Carbon monoxide (CO) gas LASER	2.6 to 4μm, 4.8 to 8.3 μm	Electrical discharge	Material processing (engraving, welding, etc.), photo acoustic spectroscopy.
Excimer chemical LASERs	193nm (ArF), 248nm (KrF), 308nm (XeCl), 353nm (XeF)	Excimer recombination via electrical discharge	Ultraviolet lithography for semiconductor manufacturing, LASER surgery, LASIK.

DYE LASER

LASER gain medium and type	Operation wavelength(s)	Pump source	Applications and notes
Dye LASERs	390-435nm (stilbene), 460-515nm (coumarin 102), 570-640nm (Rhodamine 6G), many others	Other LASERs, flash lamp	Research, spectroscopy, birthmark removal, isotope separation. The tuning range of the LASER depends on the exact dye used.

METAL VAPOUR LASER

LASER gain medium and type	Operation wavelength(s)	Pump source	Applications and notes
Helium-cadmium (HeCd) metal-vapour LASER	440nm, 325nm	Electrical discharge in metal vapour mixed with Helium buffer gas	Printing and typesetting applications, fluorescence excitation examination (i.e. in U.S. paper currency printing), scientific research.
Helium-mercury (HeHg) metal-vapour LASER	567nm, 615nm	Electrical discharge in metal vapour mixed with Helium buffer gas	Rare, scientific research, amateur LASER construction.
Helium-Selenium (HeSe) metal-vapour LASER	Up to 24 wavelengths between red and UV	Electrical discharge in metal vapour mixed with helium buffer gas	Rare, scientific research, amateur LASER construction.
Copper vapour LASER	510.6nm, 578.2nm	Electrical discharge	Dermatological uses, high speed photography, pump for dye LASERs.
Gold vapour LASER	627nm	Electrical discharge	Rare, dermatological and photodynamic therapy uses.

SOLID STATE LASER

LASER gain medium and type	Operation wavelength(s)	Pump source	Applications and notes
Ruby solid-state LASER	694.3nm	Flash lamp	Holography, tattoo removal. The first type of LASER invented; May 1960.
Neodymium YAG (Nd:YAG) solid-state LASER	1.064 μ m, (1.32 μ m)	Flash lamp, LASER diode	Material processing, range finding, LASER target designation, surgery, research, pumping other LASERs (in combination with frequency doubling to produce a green 532nm beam). One of the most common high power LASERs. Usually pulsed (down to fractions of a nanosecond).
Neodymium YLF (Nd:YLF) solid-state LASER	1.047 and 1.053 μ m	Flash lamp, LASER diode	Mostly used for pulsed pumping of certain types of pulsed Ti: Sapphire LASERs, in combination with frequency doubling.
Neodymium doped YVO ₄ (Nd:YVO) solid-state LASER	1.064 μ m	LASER diode	Mostly used for continuous pumping of mode-locked Ti: Sapphire LASERs, in combination with frequency doubling.
Neodymium doped Yttrium Calcium Ox Borate Nd:YCa ₄ O(BO ₃) ₃ or simply Nd:YCOB LASER	~1.060 μ m (~530nm at second harmonic)	LASER diode	Nd: YCOB is a so called "self-frequency doubling" or SFD LASER material which is both capable of lasing and which has nonlinear characteristics suitable for second harmonic generation. Such materials have the potential to simplify the design of high brightness green LASERs.
Neodymium Glass (Nd:Glass) solid-state LASER	~1.062 μ m (Silicate glasses), ~1.054 μ m (Phosphate glasses)	Flash lamp, LASER diode	Used in extremely high power (Terawatt scale), high energy (Mega joules) multiple beam systems for inertial confinement fusion. Nd: Glass LASERs are usually frequency tripled to the third harmonic at 351nm in LASER fusion devices.
Titanium Sapphire (Ti: Sapphire) solid-state LASER	650-1100nm	Other LASERs	Spectroscopy, LIDAR, research. This material is often used in highly-tenable mode-locked infrared LASERs to produce ultra short pulses and in amplifier LASERs to produce ultra short and ultra-intense pulses.

LASER gain medium and type	Operation wavelength(s)	Pump source	Applications and notes
Ytterbium YAG (Yb:YAG) solid-state LASER	1.03 μ m	LASER diode, flash lamp	Optical refrigeration, materials processing, ultra short pulse research, multiphase microscopy, LIDAR.
Ytterbium doped glass LASER (rod, plate/chip, and fiber)	1 μ m	LASER diode	Fibre version is capable of producing several-kilowatt continuous power, having ~70-80% optical-to-optical and ~25% electrical-to-optical efficiency. Material processing: cutting, welding, marking; nonlinear fibre optics: broadband fibre-nonlinearity based sources, pump for fibre Raman LASERs; distributed Raman amplification pump for telecommunications.
Holmium YAG (Ho:YAG) solid-state LASER	2.1 μ m	LASER diode	Tissue ablation, kidney stone removal, dentistry.
Cerium doped Lithium Strontium(or Calcium) Aluminium Fluoride LASER (Ce:LiSAF, Ce:LiCAF)	~280 to 316nm	Frequency quadrupled Nd: YAG LASER pumped, Excimer LASER pumped, Copper vapour LASER pumped	Remote atmospheric sensing, LIDAR, optics research.
Promethium 147 doped Phosphate glass ($^{147}\text{Pm}^{+3}$:Glass) solid-state LASER	933nm, 1098nm		LASER material is radioactive, one time demonstration of use at LLNL in 1987, room temperature 4 level lasing in ^{147}Pm doped into a Lead-Indium-Phosphate glass Etalon.
Chromium doped Chrysoberyl (Alexandrite) solid-state LASER	Typically tuned in the range of 700 to 820nm	Flash lamp, LASER diode, mercury arc (for CW mode operation)	Dermatological uses, LIDAR, LASER machining.
Erbium doped and Erbium-Ytterbium codoped glass LASERs	1.53-1.56 μ m	LASER diode	These are made in rod, plate/chip, and optical fibre form. Erbium doped fibres are commonly used as optical amplifiers for telecommunications.

LASER gain medium and type	Operation wavelength(s)	Pump source	Applications and notes
Trivalent Uranium doped calcium Fluoride (U:CaF ₂)	2.5μm	Flash lamp	First 4-level solid state LASER (November-1960) developed by Peter Sorokin and Mirek Stevenson at IBM research labs, second LASER invented overall (after Maiman's Ruby LASER) and liquid Helium cooled, unused today.
Divalent Samarium doped Calcium Fluoride (Sm:CaF ₂) solid-state LASER	708.5nm	Flash lamp	Also, invented by Peter Sorokin and Mirek Stevenson at IBM research labs, early 1961. Liquid Helium cooled, unused today.

SEMICONDUCTOR LASER

LASER gain medium and type	Operation wavelength(s)	Pump source	Applications and notes
Semiconductor LASER diode	Depends on device material: 0.4 μm (GaN) or 0.63-1.55μm (AlGaAs) or 3-20μm (Lead salt)	Electrical current	Telecommunications, holography, LASER pointers, printing, pump sources for other LASERs. The 780 nm AlGaAs LASER diode, used in compact disc players, is the most common type of LASER in the world.
Vertical cavity surface emitting LASER (VCSEL)	850 - 1500nm, depending on material	Electrical current	Telecommunications.
Quantum cascade LASER	Mid-infrared to far-infrared	Electrical current	Research.

OTHER TYPE OF LASER

LASER gain medium and type	Operation wavelength(s)	Pump source	Applications and notes
Free electron LASER	there exist free electron LASERs over a broad wavelength range (about 100 nm - several mm); a single free electron LASER may be tuneable over a certain wavelength range	Relativistic electron beam	Atmospheric research, material science, medical applications, missile defence.
Raman LASER , uses inelastic stimulated Raman scattering in a nonlinear media, mostly fibre, for amplification	1-2 μ m for fibre version	Other LASER, mostly Yb-glass fibre LASERs	Complete 1-2 μ m wavelength coverage; distributed optical signal amplification for telecommunications; optical solitons generation and amplification.
Nuclear pumped LASER	See gas LASERs	Nuclear fission	Research.

In welding the most common systems are CO₂/NdYAG whilst diode and fibre LASERs are now being introduced for welding and cutting [26].

Most LASERs achieved their welding task by the means of “Key-holing” technique. In this technique the beam vaporizes the material to produce a hole. This hole is filled by ionized fumes, and temperature in this hole can reach to 25, 000 °C. By moving this hole along the metal and following solidification, welding with high speed can be achieved [27].

Although LASERs in welding have the efficiency less than 15%, there are many advantages in their use [27]. Table 2-14 shows some advantages of LASER over other processes [27]. Table 2-15 shows the some of materials which can be welded by LASER [27].

Table 2-14: The advantages of LASER over other processes [27].

Competing Process	Advantages of LASER Welding
Gas Metal Arc	Faster welding rates by an order of magnitude; low distortion; no filler metal required; single-pass two-side welding.
Submerged Arc	Faster welding rates; low distortion; no flux or filler needed.
Resistance Welding	Non-contact, eliminating any debris build-up; can reach otherwise inaccessible locations; faster welding rates.
Electron Beam	Does not need to be performed in a vacuum; on-line processing; shorter cycles and higher uptimes; welds magnetic materials; does not require radiation shielding.

Table 2-15: Some of the materials which can be welded by the LASER [27].

Material	Comments
Aluminium 1100	Welds well; no cracking problem or transformation.
Aluminium 2219	No cracks; no filler metal required.
Aluminium 2024/5052/6061	Requires filler metal of 4047 Al to make hermetic, crack-free welds.
Cu-Zn Brasses	Out-gassing of Zn prevents good welds.
Beryllium Copper	Alloys containing higher percentages of alloying agents weld better due to lower reflectivity.
Copper	High reflectivity may crease uneven welds; for material less than 0.01" thick, coating may enhance weld ability.
Hastelloy-X	Requires high pulse rates to prevent hot-short cracking.
Molybdenum	Usually welds brittle; welds may be acceptable where high strength is not required.
Inconel 625	Some tendency for porosity in deep welds.
Monel	Good ductile welds; good penetration.
Nickel	Must be cleaned; good ductile welds and penetration.
Steel, Carbon	Good welds with carbon content under 0.25%; for greater Carbon content, may be brittle and crack.
Steel, Galvanized	Severe Zn boil-off causes porosity.
Steel, 300 Stainless	Welds well, except 3030 and 303SE, which crack.
Steel, 400 Stainless	Generally welds somewhat brittle; may require pre and post-weld heat treating.
Steel, 17-4PH Stainless	Needs post-weld heat treating to strengthen.
Tantalum	Ductile welds; special precautions against oxidation required.
Titanium	Ductile welds; special precautions against oxidation required.
Tungsten	Brittle welds; requires high energy.
Zirconium	Ductile welds; special precautions against oxidation required.

2-12 Diode LASER

The diode LASER is new generation of solid state LASER [28]. Some researchers indicate that the advantages of diode LASERs over traditional LASERs are [27, 28]:

- Less warming up time for starting the operation
- Less physical volume
- “High wall plug efficiency”
- Less Initial and maintenance cost
- Controllable output energy

Diode LASER normally does not operate in the ‘key-holing’ mode and material with low conductivity can easily be welded by diode LASER [27, 28]. While the Nd: YAG and Co₂ LASER work at 1.06μm and 10.6μm respectively wavelength, the diode LASER is usually operated at 810nm to 940nm in near the Infrared wavelength. This wavelength improves the “absorption rate for most of the materials” and it can be applied on both ferrous and non-ferrous material. Moreover, when “pre-coating” is imperative for heat treatment by Co₂ LASERs, It is not necessary with diode LASERs [28].

Due to reduce energy consumption for water cooling system and electrical to optical conversion, diode LASER shows good “Wall plug efficiency”, by comparison to conventional LASER [28]. Moreover, the operator of diode LASERs has more control on output energy.

2-13 Shielding gases

According to standard AS 4882-2003 normal shielding gases for welding processes are recommended. Argon, Carbon Dioxide, Helium, Hydrogen, Nitrogen and Oxygen are the common gases. Table 2-16 shows the mixtures of gases according to standard AS 4882-2003 [29].

Mason suggests that the shielding gas for LASER ablation should have high Ionisation potential [25]. Maschado & Simonelti (2000) argue that Ar, He + Ar and N₂+Ar are the best medium for LASER ablation [25].

Table 2-16: The mixtures of gases according to standard AS 4882-2003 [29].

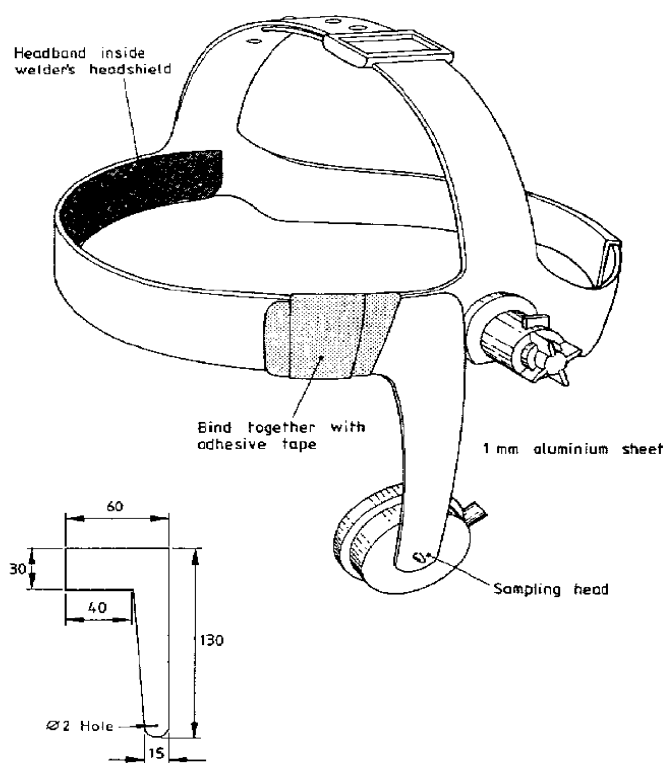
Designation	Gas mixtures (%)
SG-AC-25	Argon 75% + Carbon dioxide 25%
SG-AO-2	Argon 98% + Oxygen 2%
SG-AHe-10	Argon 90% + Helium 10%
SG-AH-5	Argon 95% + Hydrogen 5%
SG-HeA-25	Helium 75% + Argon 25%
SG-HeAC-7.5/2.5	Helium 90% + Argon 7.5% + Carbon dioxide 2.5%
SG-ACO-8/2	Argon 90% + Carbon dioxide 8% + Oxygen 2%

SG: Shielding gas

2-14 Traditional fume sampling

The recent studies on fume sampling have focused on welder's breathing zone.

Standards AS 3853-1-1990 and AS 3553-2-1990 indicate the parameters should be observed during the sampling of "Welding and allied processes" fumes [32, 33]. Some of these researches have been done in actual welding environment. Figure 2-3 shows the breathing zone fume sampler for "In-situ" sampling recommended by the Standard [32]. The result of this sampling should be reported in the form indicated in figures 2-4-a to 2-4-e [32].



All dimensions are in millimetres

Figure 2-3: The breathing zone fume sampler recommended by Standards; AS 3853-1-1990 and AS 3553-2-1990 [32].

1) BASIC DATA		Test No. 1234/A
Investigator	S. HOLMES	Operator
Date	10 DEC 1986	Company
Location	PARK LANE	Shop size
	LONDON	Ceiling height
Type of Fabrication	SMALL CYLINDRICAL STORAGE TANK APPROX 3m DIAMETER, 12m LONG	
Ventilation in use	a) Special <input checked="" type="checkbox"/> b) Local <input checked="" type="checkbox"/> XYZ GUN EXTRACTOR c) General <input checked="" type="checkbox"/> 6 FANS IN ROOF (ONLY 4 IN OPERATION) d) Natural <input checked="" type="checkbox"/> e) None <input checked="" type="checkbox"/>	
Other details	NIGHT SHIFT PRECEDED TESTS, ADDITIONAL WELDING OPERATIONS IN PROGRESS (SEE BELOW)	

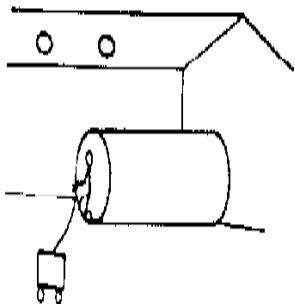
2-4-a

2) PROCESS DATA	
Type of welding or allied process	FLUX-CORED CO ₂ WELDING
Electrode or wire classification & name	2.0mm 'FABWELD DCI'
Diameter	2.0 mm
Flux or shielding gas	BASIC FLUX, CO ₂ SHIELD
Parent plate	C-Mn STEEL TO BS 4360 GRADE 43B
Coating or contaminant on wire or plate	NIL EXCEPT SOME RUSTY AREAS ON PLATE
Welding current	160 A
Arc voltage (a.c., d.c. & polarity)	20 Vac.
Wire feed speed	NOT RECORDED

2-4-b

3) SAMPLING DATA	
Time of start of shift	08.00
Operator position	KNEELING
Time of start of sampling	09.00
Headshield/handshield	1m INSIDE TANK
End of sampling	10.00
Headshield/handshield	HEADSHIELD
Arcing time/estimated percentage of sampling time	30% APPROX
Airflow through filter	Respiratory protection
a) initial	2.0L/MIN
b) final	1.9L/MIN
Type and diameter of filters	37mm 'BESTRAP' FILTER
Filter location	BREATHING ZONE
Other processes in vicinity	SUBMERGED ARC WELDING (15m DISTANT) 3 OTHER FLUX-CORED MACHINES WORKING ADJACENT TO TANK DE-SLAGGING AND GRINDING INTERMITTENTLY IN PROGRESS

2-4-c

Diagram	Additional comments
	<p>OPERATOR WORKED INSIDE TANK BACKGROUND FUME LEVELS MEASURED BOTH INSIDE AND OUTSIDE OF TANK SEE TESTS Nos 1234/B AND 1234/C</p>

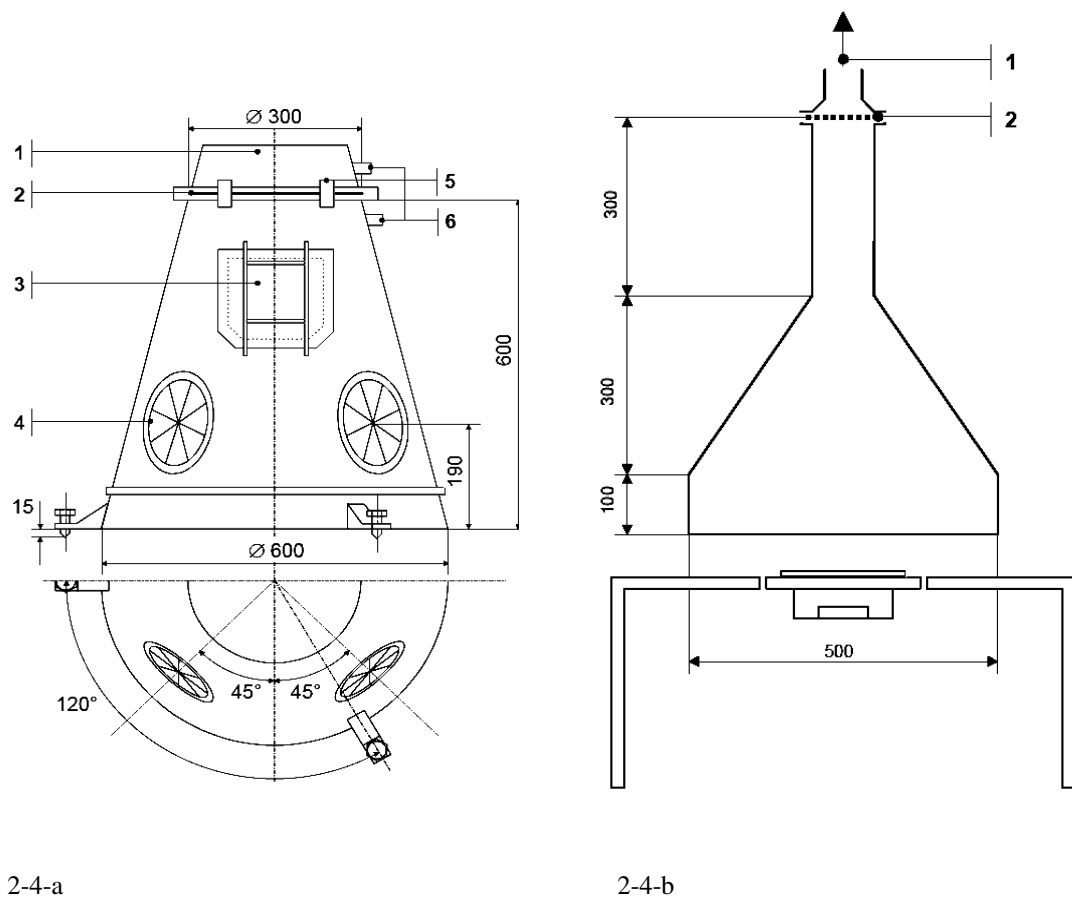
2-4-d

4) TEST RESULTS	
Fume constituents*	Concentration (in mg/m ³)
Total particulate fume
Iron
Manganese
Copper
Zinc
Nickel
Chromium
Lead
Fluoride
Others

2-4-e

Figures 2-4-a to 2-4-e: The result forms of fume sampling advised by standards; AS 3853-1-1990 and AS 3553-2-1990 [32].

Alternatively total fume sampling methods may be carried out in the laboratory and with the simulated working place. The size of chamber, filter type, flow rate, and number of experiment are advised by ISO 15011-1:2000(E) [34]. Figures 2-5-a and 2-5-b show the fume box recommended by this standard for fume analysis. Figure 2-6 shows the recommended form for reporting the results [34].



Figures 2-5-a and 2-5-b: The chamber recommended by ISO 15011-1:2000(E) for welding fume (all dimensions in millimetres) [34].

2-5-a:

1. Towards the suction system
2. Filters
3. Protection filter
4. Holes for hands and electrode holder or welding torch
5. Clamping lock system
6. Couplings for the measure of load loss [34]

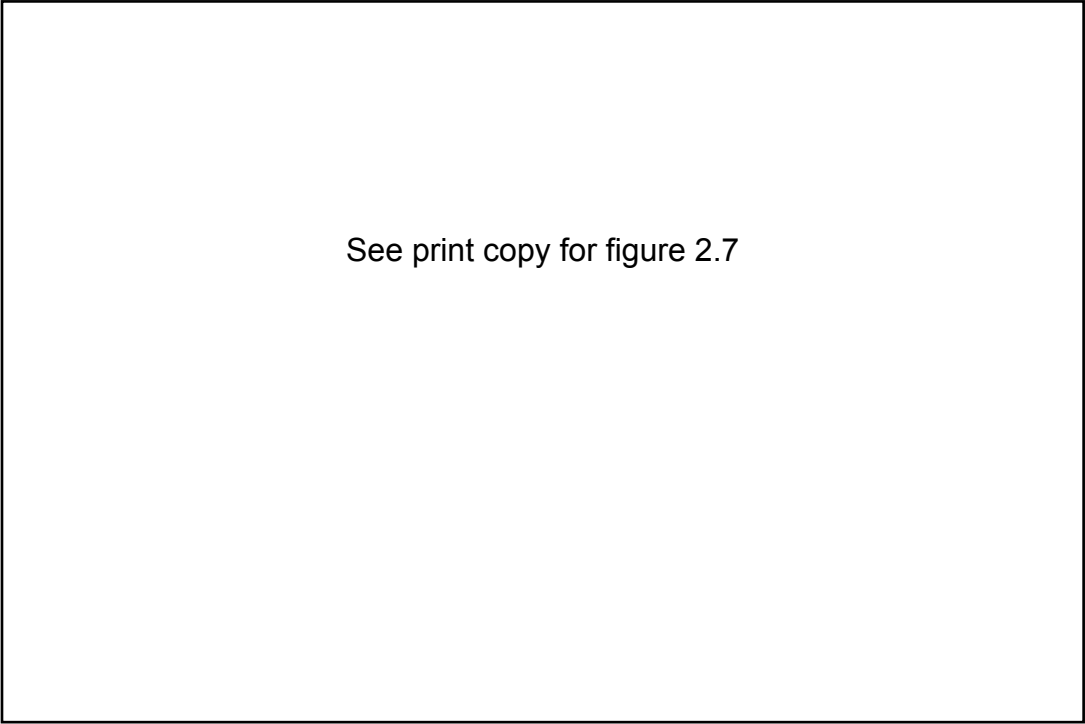
2-5-b:

1. towards the suction system
2. Fume box

Date of test	Operator		Ref.			
Process			Type of fume box			
Welding position						
Consumable	Manufacturer/brand name					
	Consumable name		Standard			
	Batch					
	Diameter					
	Remarks					
Test piece	Base metal					
	Dimensions		Standard			
	Surface conditions					
	Remarks					
Shielding gas	Trade name					
	Composition		Standard			
	Flow rate					
	Remarks					
Welding and monitoring equipments	Power source: Trade mark and complete type					
	Recording equipment					
Measurement details	Test 1	Test 2	Test 3	Test 4	Test 5	Units
Welding : manual/mechanized						
Arc voltage – Polarity						V/DC(+)DC(-)AC
Arc current						A
Pulsing details (where applicable)						
Wire feed speed (where applicable)						m/min
Stick out (where applicable)						mm
Welding speed						cm/min
Remarks						
Arc time						s
Filter weight						mg
after test						mg
before test						mg
Particulate fume weight						
Mean value of emission rate						mg/s
Welding fume composition of elements						%(m/m)
Other remarks:						

Figure 2-6: The ISO 15011-1:2000(E) recommended form for reporting the fume sampling results [34].

Moreover, some researchers designed new kind of chambers which can meet their objectives in experiment. Gael Ulrich, et al. designed a chamber for analysis the particle size of the fume at the University of New Hampshire (figure 2-7). This chamber is coupled with vacuum pump, arc welding instruments and fume collector [35].



See print copy for figure 2.7

Antonini, et al. designed a comprehensive robotic fume generator (figure 2- 8) at National Institute for Occupational Safety and Health, West Virginia. The devices were employed in order to generate and investigate the fume emission comprised [36]:

- Enclosed control room
- Six-axis robotic arm
- Wire feeder
- Torch cleaner
- Coolers
- Base metal holder
- Animal exposure chamber
- Gas characterization devices



See print copy for figure 2.8

1. Enclosed control room including the welding power source and controller
2. Robotic welding fume generators that contains the six-axis robotic arm, wire feeder, torch cleaner, coolers, and base metal holder.

2-15 Particle size and morphology

Fumes and particulate which generated during the welding are normally in the range of 0-2 μ m dimension while some of those can be agglomerated up to 10 μ m [1].

Je Yu, et al. launched a study on fume generated from the MMA of Stainless steel. Fumes were sampled from this process every 15min with flow rate of 2L/min and analysed using a Transmission Electron Microscope (TEM) [37]. Figure 2-9 shows the logarithmic diagram of distribution of fume versus particle size (aerodynamic diameter) [37]. Figure 2-10 shows Mass concentration of fume versus the particle size (aerodynamic diameter) [37].

Particles with size less than 0.1 μ m are called “Ultra-fine” [38]. As reported in Metal-Berufsgenossenschaft the size and morphology of particles are shown in table 2-17 [38].

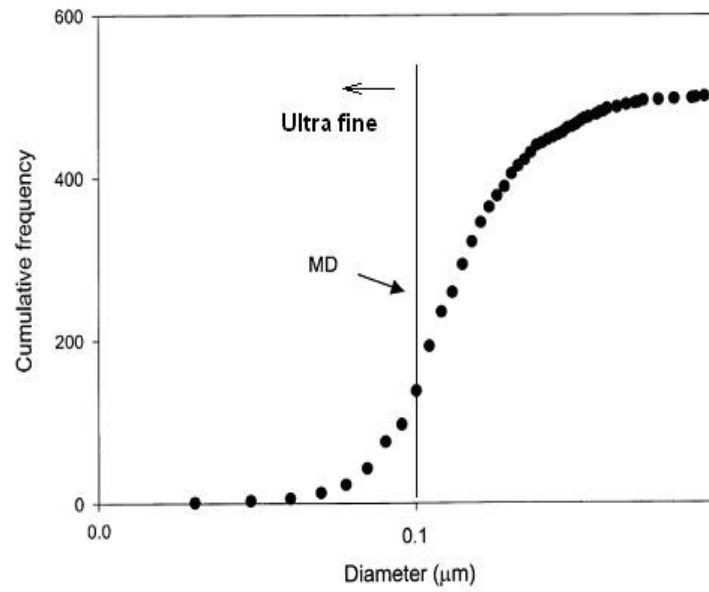


Figure 2-9: The logarithmic diagram of distribution of fume versus particle size [37].
MD: Mean Diameter

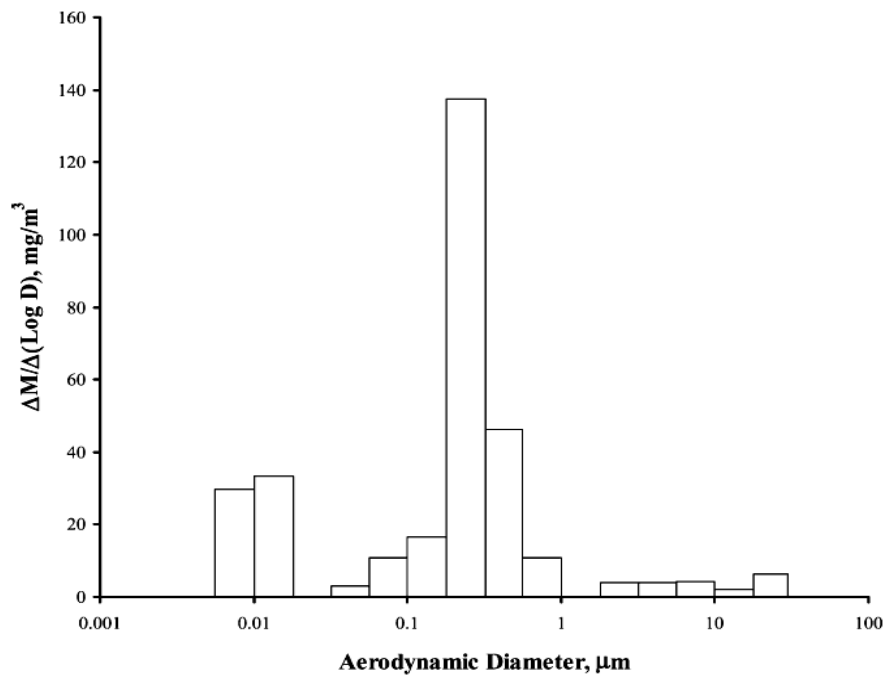





Figure 2-10: The mass concentration of fume versus the particle size (Aerodynamic diameter) [37].

Table 2-17: Morphology and size of the fume particle in the MMAW, GMAW, MIG and TIG [29].

Process	Material	Particle			
		Form of individual particles	Size		
			Individual particles	Chains	Agglomerates
			(Diameter)	(Length)	(Diameter)
Manual metal arc welding with covered electrodes MMA	Cr Ni steel	spherical shape	up to 50 nm	several μm	up to 500 nm
			up to 400 nm	several μm	
Gas shielded arc welding MAG/MIG	Cr-Ni-steel	spherical shape	up to 10 nm	up to 100 nm	up to 100 nm
	Aluminium alloys	spherical shape	10 to 50 nm up to 400 nm	n. i. n. i.	n. i.
					
n. i. = no indications μm = Micrometer ($1 \mu\text{m} = 10^{-3} \text{ mm} = 10^{-6} \text{ m}$); nm = Nanometer ($1 \text{ nm} = 10^{-6} \text{ mm} = 10^{-9} \text{ m}$)					

The studies regarding ultra fine particles have been carried out with arc processes and particularly consumables. Table 2-18 comprehensively shows the chemical compositions of Arc welding fumes which are evaluated by the X-Ray, STEM and SPEC [29].

Table 2-18: The chemical compositions of Arc welding fumes [29].

MMA ¹⁾ with unalloyed electrode (E6010); Composition according to category			
Main category	Percentage of particle number (%)	Mean diameter in μm	Composition (%)
Fe/low Si	31	0,188	Si(36) Mn(4) Fe(56)
Fe/high Si	10	0,245	Al(21) Si(46) K(9) Fe(21)
Fe-Mn	16	0,202	Si(36) Mn(14) Fe(44)
Ca-Fe	8	0,169	Si(37) Ca(13) Fe(43)
MMA ¹⁾ with unalloyed basic electrode (E7018); Composition according to category			
Main category	Percentage of particle number (%)	Mean diameter in μm	Composition %
K-Fe	14	0,179	Si(18) K(36) Fe(28)
Ca-Fe	15	0,158	Al(7) Si(17) Ca(25) Fe(37)
K-Ca-Fe	48	0,188	Al(4) Si(10) K(28) Ca(22) Fe(23)
MAGC ²⁾ with low alloy solid wire (E70S-3); Composition according to category			
Main category	Percentage of particle number (%)	Mean diameter in μm	Composition (%)
Fe	9	0,153	Si(7) Fe(90)
Fe/low Si	14	0,173	Si(19) Mn(6) Fe(76)
Fe-Mn	17	0,129	Si(12) S(4) Mn(13) Fe(62)
Fe-Cr	5	0,129	Si(16) Cr(10) Fe(53) Zn(5)
Fe-Al	6	0,103	Al(18) Fe(69)
K-Fe	6	0,111	Si(6) K(16) Mn(6) Fe(58)
Ca-Fe	10	0,118	Al(7) Si(13) Ca(15) Mn(5) Fe(48)
Fe-reich	8	0,148	Al(4) Si(5) K(6) Fe(71)
MAGM ³⁾ with low alloyed flux-cored wire (E70T-1); Composition according to category			
Main category	Percentage of particle number (%)	Mean diameter in μm	Composition (%)
Fe	14	0,140	Fe(99)
Fe/low Si	25	0,160	Si(25) Fe(72)
Fe-Mn	37	0,178	Si(8) Ti(11) Mn(19) Fe(59)
MMA ¹⁾ with high alloy Cr/Ni electrode (E308-16); Composition according to category			
Main category	Percentage of particle number (%)	Mean diameter in μm	Composition (%)
Fe-Mn	5	0,166	Si(32) Ti(5) Mn(26) Fe(26)
K-Cr	5	0,155	Al(6) Si(19) K(31) Cr(17) Mn(9)
K-Fe	18	0,169	Si(22) K(27) Mn(10) Fe(22)
K-Cr-Fe	5	0,176	Si(14) K(28) Ti(10) Cr(24) Fe(21)
Ca-Fe	7	0,144	Si(24) Ca(18) Mn(12) Fe(23)
K-Ca-Fe	7	0,159	Si(25) K(20) Ca(15) Mn(6) Fe(17)
K-Mn	8	0,161	Al(6) Si(25) K(29) Mn(22)
K-reich	7	0,174	Si(26) Cl(5) K(50) Ca(5)
Si-reich	6	0,161	Si(56) S(8) K(8)
MIG with Al containing solid wire (E5356); Composition according to category			
Main category	Percentage of particle number (%)	Mean diameter in μm	Composition (%)
Al	86	0,327	Al(99)
Al-Cu	7	0,318	Al(65) Cu(35)

MMA: Manual Metal Arc Welding
MAGC: MAG with shielding gas CO₂
MAG: MAG with gas mixture Ar/CO₂

2-16 Factors that effect fume generation

Slater (2004) Reviews the factors that affect the amount, type morphology and shape of the fumes generated during the arc welding, these are [1]:

- Electrode
 - Composition
 - Coating
 - Size
 - Type
- Shielding Gas
 - Composition
 - Consumption
- Welding Parameters
 - Voltage
 - Current
- Base metal
 - Composition
 - Coating
- Welding speed
- Welding geometry
- Welding processes

Considering the interest of this thesis, shielding gas and base metal are the most important factors which are described as below:

2-16-1 Shielding gas

The gases with higher ionisation potential are recommended for ablation even though; the selection of gas for ablation should be done with regards to its mass, reactivity and Ionisation potential altogether [25].

Table 2-19 shows the Ionisation potential of active and inert gases [25].

Irving (1992) indicates that the existence of CO_2 in shielding gas, owing to its lower disassociation energy, increases the amount of generated gases [1]. In similar, the higher flow rate of shielding gas, increase the amount of fumes [1].

Table 2-19: The Ionisation potential of active and inert gases [25].

Buffer gas	Ionisation Potential(ev)	Reaction Gas	Ionisation Potential(ev)
He	24.6	H ₂	15.4
Ne	21.6	H ₂	13.6
Ar	15.8	N ₂	15.7
		CH ₄	12.6
		NH ₃	10.2
		O ₂	12.2
		H ₂ O	12.6
		Xe	12.1

In present work the influence of common welding gas mixture is a key objective and in the first instance the effect of oxidizing potential is to be determined. For this reason Helium, Argon with Oxygen addition are of interest.

2-16-2 Base metal composition

In welding the base metal composition is probably of less importance than that of the consumable but in this case the target material is required to stimulate evaporation from the consumable [1].

Along side with these factors, the effect of LASER parameters on fume generation has yet to be determined.

2-17 Sample analysis

In accordance with AS 3853.2-1991, “Fume from welding and allied processes”, the numbers of advised methods for analysis of gases are reported [33]:

- Detector tubes (for short term and long term)
- Instrumental methods
 - Dispersive and non-dispersive Infrared absorption
 - Diffusion of carbon monoxide
 - Gas chromatography
 - Colometric or amperometric determination of Iodine
 - Photometry of chemiluminescence with Ethylene
 - Absorption of Ultra Violet radiation
- Chemical methods

- Oxidation of Potassium iodide
- Oxidation of Dimethoxystibene in Tetrachloroethane to produce Anis Aldehyde
- Absorption in Sodium hydroxide
- Absorption in Barium hydroxide

Jenkins & Eager (2000) suggest that regarding to size range of particles the analytical method varies [35].

Table 2-20 shows the different analytical methods for different size range of welding particles [35].

Table 2-20: The different analytical methods for different size range of welding particles [35].

Characterization method	Size range (µm)	Detection limit notes (NA = not applicable)	Notes
Particle Size Distribution Impactors (various types)	0.1–20	NA	Size distribution by mass chemically analyse size groups.
Electric Aerosol Analyser (EAA) and differential mobility particle sizer	0.01–1	NA	Size distribution by number.
Aerodynamic particle sizer	0.1–25	NA	Size distribution by number.
Scanning Electron Microscope (SEM); High Resolution (HRSEM)	0.5–50 0.002–1	NA	Particle sizes can be measured from micrograph.
Electron Probe Microanalysis (EPMA)	0.5–50	NA	Particle sizes can be measured from micrographs.
Transmission Electron Microscope (TEM)	0.001–1	NA	Particle sizes can be measured from micrograph.
Light microscopy	1–400	NA	
Elemental Composition X-ray Fluorescence spectrometry (XRF)	bulk	100 ppm	Atomic numbers >10 very fast.

Characterization method	Size range (μm)	Detection limit notes (NA = not)	Notes
Neutron Activation Analysis (NAA)	bulk	0.01%	Atomic numbers >10 requires nuclear reactor.
Optical emission spectrometry and mass spectrometry	bulk	1–10 ppm	Atomic numbers >10.
Atomic Absorption Spectrometry (AAS)	bulk	10 ppm	
Energy-Dispersive Spectrometry with SEM (SEM-EDS)	1–50	0.1%	Atomic numbers >10.
Wavelength-Dispersive Spectrometry with EPMA (EPMA-WDS)	1–50	0.1%	Atomic numbers >4.
Energy-Dispersive Spectrometry with TEM (TEM-EDS)	0.01–0.5	0.1%	Atomic numbers >5, scanning TEM can map element distribution at nm resolution.
Proton-Induced X-ray Emission spectrometry (PIXE)	>5	0.1%	Atomic numbers >10.
LASER Microprobe Mass Spectrometry (LAMMS)	>1	10 ppm	All elements.
Secondary Ion Mass Spectrometry (SIMS)	>5	10 ppm	Light element capable.
Auger Electron Spectrometry (AES)	>0.1	0.1%	Atomic numbers >3 lower sample must be conductive.
X-ray-induced Photo-electron Spectrometry (XPS or ESCA)	>5	0.1%	Surface composition (3–5 nm deep) (XPS or ESCA) contamination error common.

Characterization method	Size Range (µm)	Detection limit notes (NA = not applicable)	Notes
Chemical Speciation X-ray Diffraction (XRD)	bulk	NA	Only of crystalline material; particles must be >0.05 µm or they will seem amorphous.
X-ray-induced Photoelectron Spectrometry (XPS or ESCA)	bulk	NA	Need appropriate standards (XPS or ESCA) Collect on non interacting filter.
Selected Area Electron Diffraction with TEM (TEM-SAED)	~0.3	NA	Only of crystalline material.

CHAPTER THREE

EXPERIMENTAL PROCEDURE

3-1 LASER ablation chamber design

3-1-1 Objectives

The objective of this work was to enable metal fume to be produced in a controlled atmosphere. Due to the high LASER power used the enclosure was required to satisfy the safety requirements of AS/ 2211.6:2002.

The chamber was designed to incorporate:

- A CCD camera/ online spectroscope
- The LASER head (focussing lens)
- Shielding gas input
- A fume collector

Initial drawings were completed with AutoCAD, 2005, according to Australian standard AS 1100.201-1992.

3-1-2 Chamber design

The initial design was based on a main vertical body with cylindrical shape and two oblique inputs on the sides of cylindrical shape. Figure 3-1 shows a sketch of chamber main body.

On the top face an adaptor attaches a fume collector to chamber, on one side of the tube an adaptor attaches the CCD camera, and on the other side an adaptor attaches the combined adaptor for both shielding gas and LASER head.

The adaptor for LASER head comprised:

1. A main cylindrical body welded at the bottom to a circular plate with a hole in the size of cylinder in middle.
2. The circular plate was grooved round the hole in order to let the gas feed inside. This flow of the gas into the chamber prevents the fume flows towards the face of the focussing lens which could result in damage to the LASER head.
3. A spacer to hold the protective cover glass.
4. A gasket for the LASER protective lens.

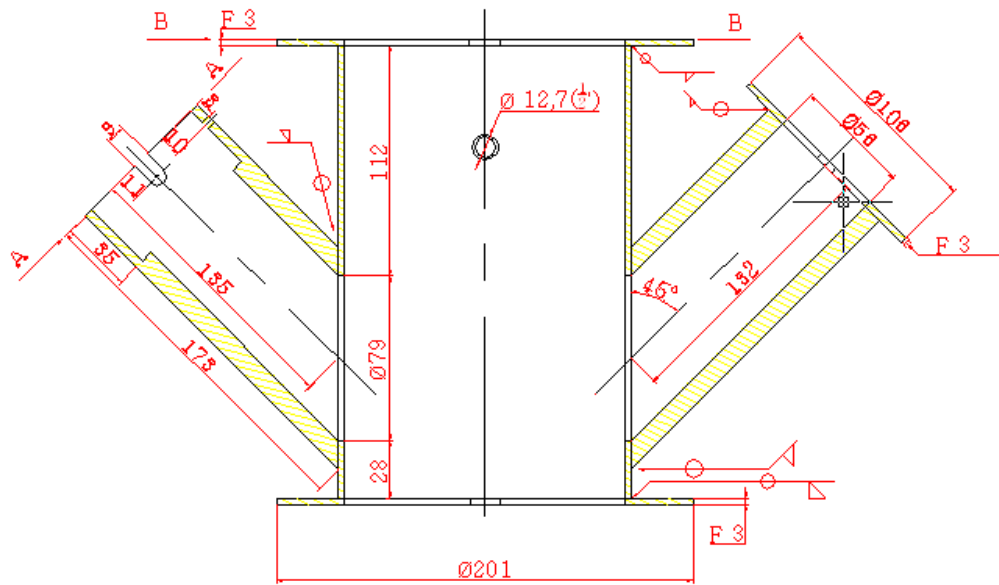


Figure 3-1: The initial sketch of ablation chamber.

3-1-3 Prospective materials and dimensions

The potential materials selected for this design were Stainless Steel for main body and Aluminium for adaptors and accessories.

The dimensions were calculated in such a way as to ensure the 200mm focal length from the LASER head to sample could be achieved.

3-1-4 Safety issues

Because the LASER device is used in present work is a powerful LASER with potential to cause serious hazards, all of the welds were designed as continuous seam welds. The main chamber body was also designed to be mounted on a Copper slab seat which would act as a LASER 'dump' in the event of failure.

3-2 New chamber adaptation

The manufacturing of the device described above was investigated in collaboration with UOW workshop staff and the design was optimised to aid manufacturing. However, due to resource commitments it was envisaged that delivery would be protracted. To enable the project timescales to be met an existing chamber was located and adapted for this application. The chamber which was used had the potential to be adapted for LASER ablation purposes. Figure 3-2 shows the existing chamber prior to adaptation.

The Chamber comprised:

- Main cylindrical Stainless Steel body
- Four inputs at one end perpendicular to main body and an open end
- An adjustment mechanism at one end allowed the sample holder to be moved longitudinally along the horizontal axis of the chamber

In order to adapt this chamber for LASER ablation purposes firstly, it had to be mounted on a mobile trolley secondly, the adaptor panels for the LASER head, CCD camera and gas feed and fume collector had to be designed. Figure 3-3 shows the basic chamber and its mobile trolley.

A CCD camera adaptor was designed as a circular plate the same size as one chamber input port with a drilled hole in middle for the CCD camera. On the inside of the adaptor a holder for a filter to be mounted in front of the CCD lens was designed. This adaptor was designed to attach to the chamber with three clamps at a spacing of 120°. Figures 3-4-a and 3-4-b show the CCD camera adaptor.

The gas feed consisted of a circular plate with hole in middle for threaded hose connection. On the inside face of the adaptor a barrier was designed in order to prevent the interruption in natural movement of fume due to the flow of the chamber gas. This adaptor was again designed to attach to the chamber with three clamps. Figures 3-5-a and 3-5-b show the shielding gas feed adaptor.

For LASER head adaptor the following parts were designed:

- A main cylindrical body seam welded in the middle to a flange .The flange attaches to chamber input port.
- On the top a groove was designed for a metal gasket and spacer for the protective LASER cover glass.

The fume collector adaptor on the top was designed as a simple circular plate with a hole in middle for filter holder. The filter holder used was a standard 25mm breathing zone sampler head. Figures 3-6-a and 3-6-b show the fume collector adaptor.

Figures 3-7-a to 3-7-e show the main body, flange, spacer and protective lenses of LASER head adaptor.

A schematic cross section of the assembly showing the juxtaposition of the items described above is shown in figure 3-8.

Due to safety concerns a mobile safety cover was designed to cover the whole chamber to cater for the unlikely but possible failure of the vessel seals or ports and the resultant escape of IR radiation. Figures 3-9-a and 3-9-b show the mobile safety cover for chamber. Figures 3-9-c and 3-9-d show the chamber with the safety cover removed.

The LASER which was employed for this work was a 3kW, 8 stack Diode LASER, LDF 1000-3000, serial A331671, VG5 from *Laserline*. The LASER out put was coupled to the LASER rig by an optical fibre.

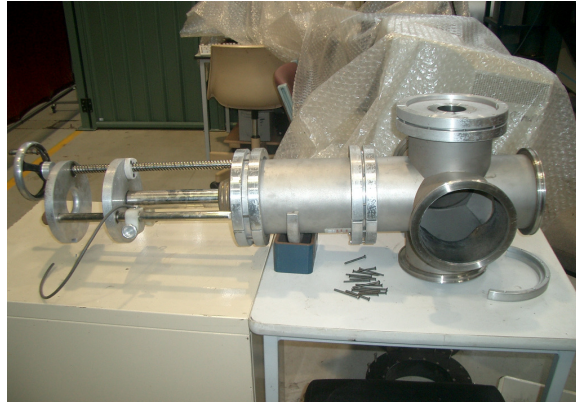


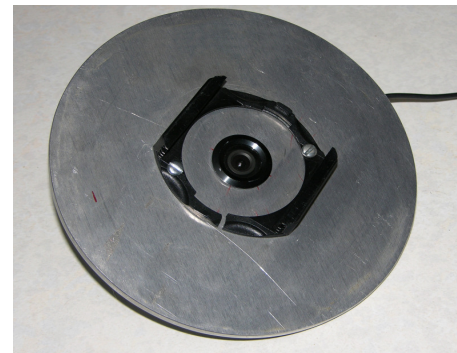
Figure 3-2: The basic Chamber.



Figure 3-3: The basic chamber and its mobile trolley.



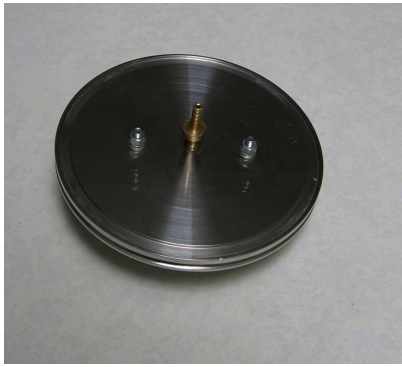
3-4-a



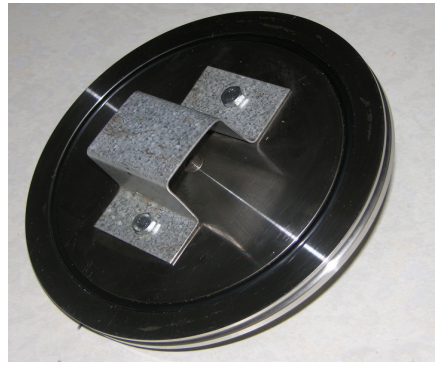
3-4-b

Figure 3-4-a: The CCD camera as installed on its adaptor

Figure 3-4-b: The inside view of CCD camera adaptor and the holder for bond pass filter and protective lens.



3-5-a



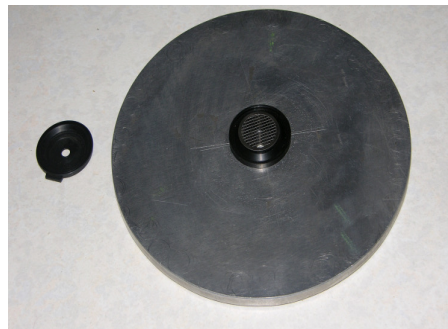
3-5-b

Figure 3-5-a: The outside view of shielding gas feeder adaptor and hose barb.

Figure 3-5-b: The inside view of gas feeder adaptor and the gas barrier which deflects the stream of shielding gas.



3-6-a



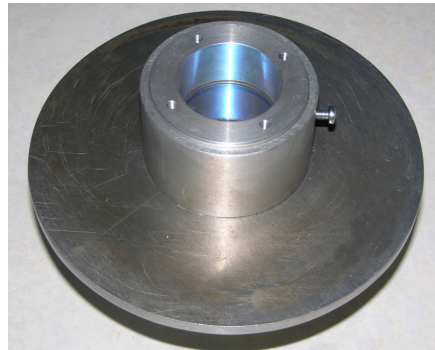
3-6-b

Figure 3-6-a: The inside view of fume collector adaptor.

Figure 3-6-b: The outside view of fume collector adaptor, the filter holder net and its cap.



3-7-a



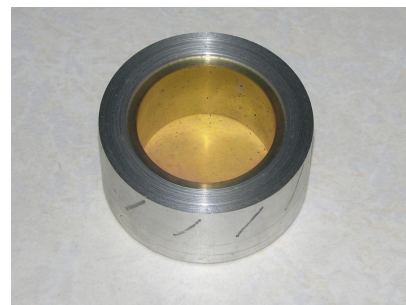
3-7-b



3-7-c



3-7-d



3-7-e

Figure 3-7-a: The outside view of LASER head adaptor where the LASER head can be fixed with bolt.

Figure 3-7-b: The inside view of LASER head adaptor where the LASER protective lens is fixed.

Figure 3-7-c: From right to left; the protective lens spacer, the protective lens, the protective lens metal gasket where the lens seats on and LASER head main body adaptor.

Figure 3-7-d: The protective lens spacer.

Figure 3-7-e: The protective lens spacer and the protective lens seated in the groove.

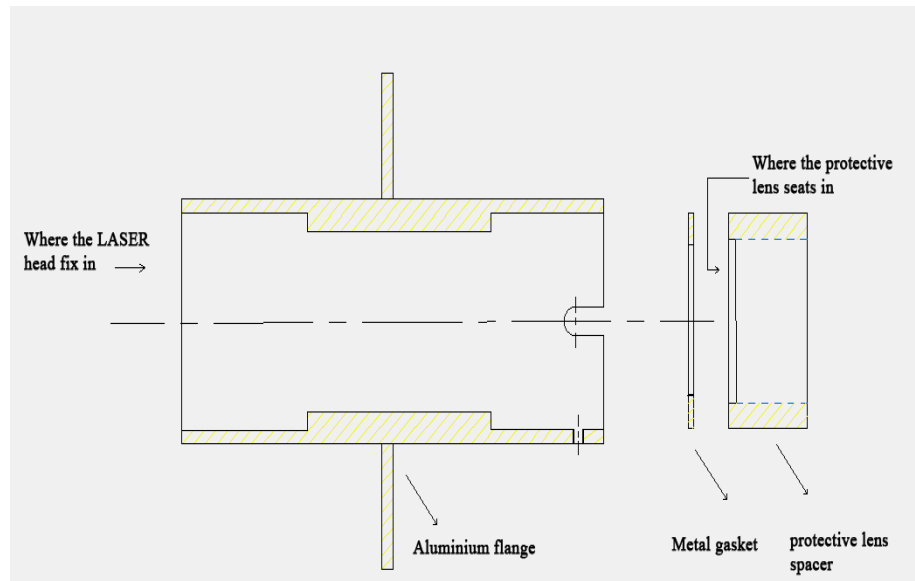
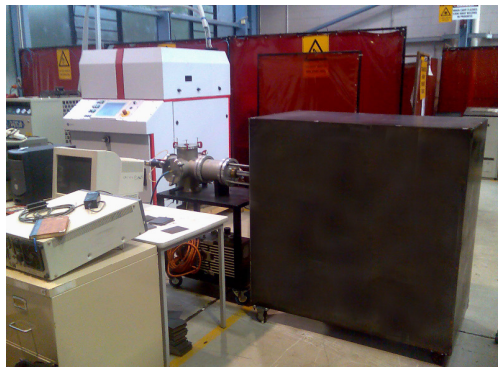


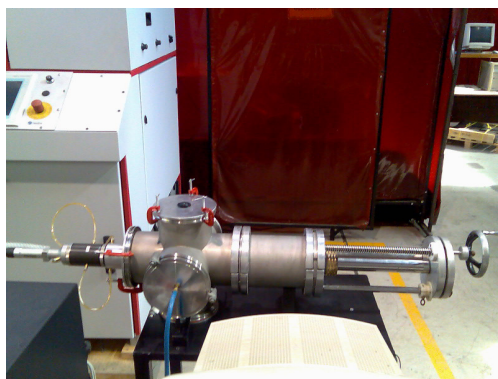
Figure 3-8: A schematic cross section of the assembly showing the juxtaposition of the different parts of LASER head adaptor.



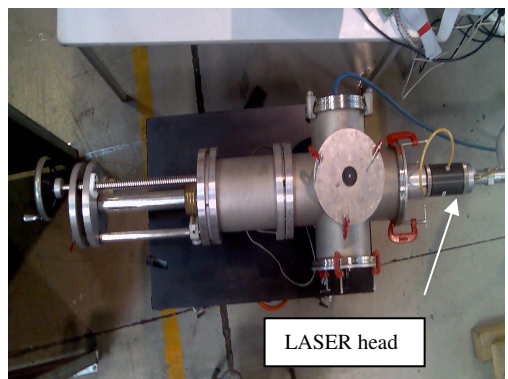
3-9-a



3-9-b



3-9-c



3-9-d

Figure 3-9-a and 3-9-b: The mobile safety cover for Chamber.

Figure 3-9-c and 3-9-d: The chamber with the safety cover removed.

3-3 Sampling method

The target specimen for ablation was plain carbon steel in all experiments. The size of the specimen was 122mm * 95mm by 2mm thickness.

After a few trials run with the new chamber it was found that insufficient fume could be collected on the filter on the fume collector panel due to the low amount generated and large size of the chamber. Therefore, a new sampling method was established.

Because of the natural buoyancy of the fume, it was attempted to use an Aluminium foil above of the metal sample to collect the fume. After few trials it was observed that the fume can penetrate the gap between Aluminium and metal sample. In order to solve this problem and after some trials and errors a more reliable technique was developed, this involved:

1. Cleaning the metal sample underneath the Aluminium sheet with Acetone.
2. Placing the Aluminium sheet on the top of the sample half folded onto the back of the metal sample.
3. Cleaning the Aluminium sheet with Acetone.
4. Placing two parallel holder bars to avoid separation of the Aluminium sheet.

In order to maximize the amount of fume collected on the Aluminium sheet the distance between the bottom border of Aluminium sheet and the LASER spot was minimized.

The application of a LASER for fume generation by ablation is a novel Idea. Therefore, establishing the characteristics of the ablation device and examining the repeatability of experiments were the priorities of this work.

3-4 LASER spot size output

The focal length of the LASER focussing lens was 200mm and the system was designed to allow the LASER to be focussed on the sample surface at the midpoint of the sample adjustment. However, due to tolerance variations in the set up it was necessary to check the focal position accurately. When the LASER is focussed at the surface of the sample the focal spot size is minimised and the highest power density is achieved.

The system needed to be calibrated and the minimum spot size produced by the LASER on the sample surface and its relation with sample position adjustment needed to be determined experimentally. The position of the sample relative the LASER lens was adjusted over a distance of 40mm in 2mm steps. To assess reproducibility each of the experiments was carried out at least four times. The LASER powers chosen for these experiments were 300W and 500W.

3-5 Weighing experiments

In order to examine the generated fume weight, a weighing technique was established. In this technique the air flow and balance of the Aluminium foil on the scales and standard deviation of the scale were also investigated. The precision scales used for this experiment was a six digit *Sartorius* unit.

Since the different ways of folding the Aluminium foil affect the airflow and balance readings, different ways of folding the Aluminium foil were examined. The best pattern is shown schematically in figure 3-10. The Aluminium sheet is first folded around axis number 1 then two and finally 3 to reach to maximum stability.

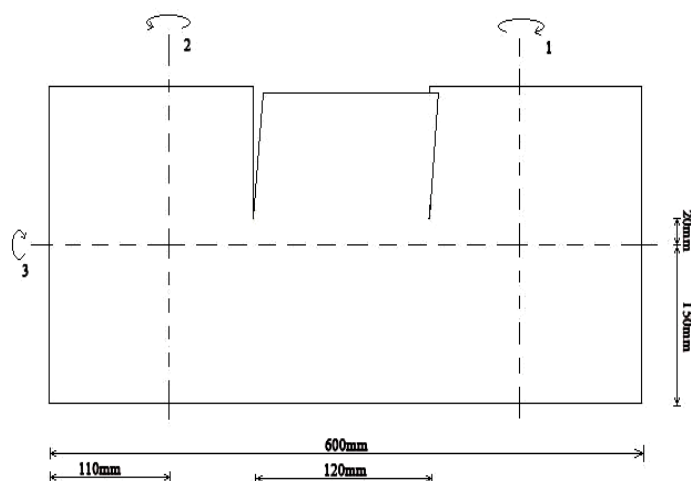


Figure 3-10: The folding pattern, Aluminium foil should be folded initially around axis number 1 then 2 and finally 3.

3-6 Generating fume weight Vs. Focal length in different atmospheres

In order to determine the weight of generated fume the following parameters were kept constant during the experiments:

- The distance between the bottom border of Aluminium sheet and uppermost LASER striking spot
- The dimensions of Aluminium sheet

The weighing protocol; carried out in sequence as below:

- Wiping the Aluminium sheet with Acetone
- Cutting the specified pattern. Figure 3-11 shows the Aluminium foil cutting pattern and metal sample

- Folding the Aluminium sheet to the specified pattern
- Putting it on scales and allowing the reading to stabilize for 15 sec
- Reopening it and installing on metal sample
- Wiping the Aluminium sheet with Acetone
- Seating the metal sample inside the chamber on the sample seat. Figure 3-12 shows the seat for sample inside the chamber.
- Attaching the adaptor to the chamber with three clamps at a spacing of 120°
- Sliding the safety cover to cover the chamber
- Plugging the vacuum pump (AEG, Spezial,92500081) and let it run for 4 min (For purge the chamber with different atmosphere)
- Striking the LASER for 15 or 30 sec
- Removing the Aluminium sheet from metal sample. Figure 3-13 shows the Aluminium foil, holder bar and generated fume after removed from chamber.
- Folding the Aluminium foil as the same pattern of figure 3-10
- Weighing the sample , again with 15sec time for the reading to stabilize
- Temporarily storing the sample as it is folded in clean, dry sterilized bag. Figure 3-14 shows the Aluminium foil while it is temporarily stored in the bag.
- Maintain all the samples in a desiccator

To survey the repeatability of experiments for specific LASER power, atmosphere and time of striking the experiments were repeated for five times.

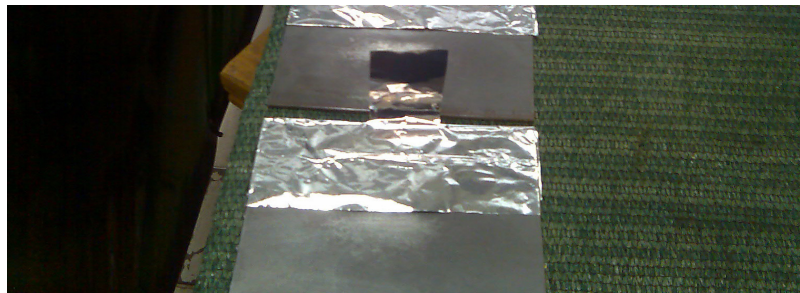


Figure 3-11: The Aluminium foil cutting pattern and metal sample.

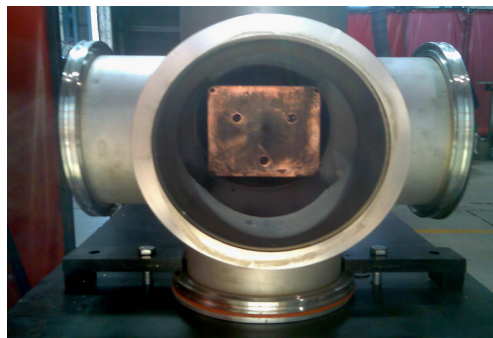


Figure 3-12: The sample seat inside the chamber.



Figure 3-13: The Aluminium foil, holder bar and generated fume after removed from chamber.



Figure 3-14: The Aluminium foil while it is temporarily stored in the bag.

3-7 Generating fume weight Vs. LASER power in different atmospheres

The sampling was carried out in four different atmospheres:

1. Air
2. CO_2
3. Stainshield 66
4. Argoshield 52

The above gases chemical description are shown in table 3-1 (Reference: *BOC*; www.boc.com.au).

Table 3-2 shows the different conditions under which the fume weight experiments were carried out.

Table 3-1: The chemical description of applied shielding gases.

Shielding gas name*	Industrial Grade code	Content	Purity	Size
Carbon Dioxide		Co ₂	>99.9%	G
Argoshield™ 52	070	Co ₂	25%	G
		Ar	Balance	
Stainshield™ 66	093	H ₂	1%	G
		Co ₂	2.8%	
		Ar	Balance	

*Reference: BOC; www.boc.com.au

Table 3-2: The summary and reference numbers of the different conditions used.

Focal Length (mm)					Time of striking
LASER power (W)		210	200	190	
	100	#1	#2	#3	15 Sec
	300	#4	#5	#6	
	500	#7	#8	#9	
	300	#11	#18	#19	30 Sec
	500	#20	#21	#22	
	300	#17	#12	#13	30Sec
	500	#14	#15	#16	
	300	#23	#24	#25	30 Sec
	500	#26	#27	#28	

Atmosphere

	Air
	Co ₂ (gas code:081, size: G)
	Argoshield 52 (gas code: 070, size G)
	Stainshield 66 (gas code:093, size G)

Sample numbers for the SEM reference

3-8 Analyses

Scanning Electron Microscopy (SEM) and Transmission Electron Microscopy were chosen for analysis of the particulate morphology and size distribution. Also, Energy Dispersive spectroscopy (EDS) and Scanning Transmission Electron Microscopy (STEM) are the methods which were chosen for chemical analysis.

3-8-1 SEM

The SEM experiments were done with *Leica stereo scan 440 SEM*. The *Leica steroscan* includes two parallel computers. The main computer does the Imaging and the parallel system generates the Energy Dispersive spectroscopy (EDS) results.

3-8-1-1 Sample preparation and Imaging

The methodology for capturing the image with the SEM is as follow:

1. Provide a stub holder with capacity of holding at least 15 stubs. This stub holder should be fitted inside the desiccator. For the present work this stub holder was designed to be a thick cardboard disc with circular patterned holes. Figure 3-15 shows the desiccators contains stub-holders and stubs ready for the SEM.
2. Wash a stub with Ethanol while it is being held with tweezers
3. Fix the stub on the stub holder
4. Wash the scissors and tweezers with Ethanol to prevent charging the Aluminium foil
5. Cut the conductive double sided tape in square shape (10*10mm) while the double sided tape is held with tweezers. Figure 3-16 shows the SEM stub and double-sided tape.
6. Stick the double sided tape on the clean stub
7. Wash the scissors and tweezers with Ethanol
8. Cut the Aluminium foil in square shape 8*8mm while the Aluminium foil is held with tweezers
9. Stick the Aluminium foil on the stub. In order to capture a good picture the Aluminium foil should be flat on the stub.
10. Fix the stub inside the SEM chamber on the stub holder with tweezers while the fabric gloves are put on. Figure 3-17 shows the stub holder inside the SEM chamber.
11. Pump out the chamber By using the 'Vacuum' button on right bottom of screen
12. Turn the beam on by using the 'beam' button on right bottom of screen when the chamber was vacuumed
13. Set the 'I-probe' to 50 pA and adjust the 'brightness' to the level which the stub holder inside the chamber can be seen. By choosing the Probe button from software toolbar 'I-probe' can be adjusted with right click and scroller and brightness with middle mouse click and scroller.
14. Set the magnification to the level the annotation bar shows the length of 2 micrometres

15. Reach the best resolution and depth of field by adjusting the working distance. Working distance can be changed with choosing the magnification button on toolbar menu and using the middle mouse click and scroller. The best resolution can be achieved by minimizing the 'I-probe' and Working distance.
16. save the Image by using the Save button on the File/menu



Figure 3-15: The desiccator contains stub-holders and stubs ready for the SEM.



Figure 3-16: The SEM stub and double-sided tape.

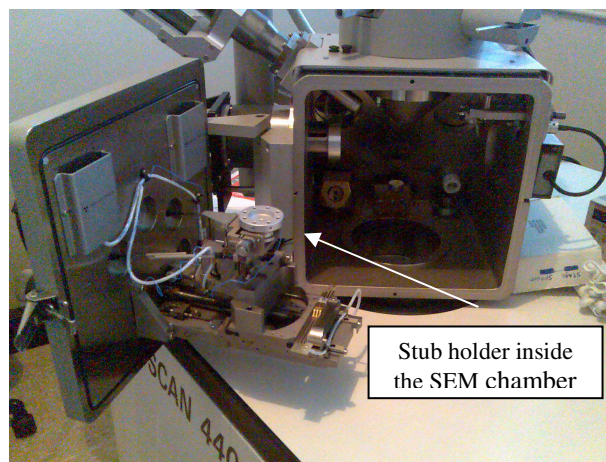


Figure 3-17: The stub holder inside the SEM chamber.

3-8-1-2 EDS analysis

When the Imaging process is completed, the X-ray collector should be adjusted to nearest distance inside the chamber. The screwing bar outside of the chamber allows the operator adjust this distance. Figure 3-18 shows the X-ray device adjustor outside the SEM chamber.

The following steps should be followed to obtain map of elements and energy dispersive spectrum:

1. Turn on the 'exposure off' from the toolbar menu. This function helps the parallel system, The EDS software, *Link ISIS*, simultaneously receives the SEM Image.
2. Adjust the 'I-probe' in the main computer to the level that the capturing 'Dead time' on the EDS system reaches to 25%
3. Save the spectrum which is obtained during the capturing life time by using the Save button from File menu
4. Label the peaks of spectrum using button which is shown as a question mark on the EDS software box. This feature helps to recognize the elements of the peaks of spectrums.
5. Use the paint button from the EDS software box and choose all recognised elements
6. Turn the map of elements button from toolbar menu
7. Allow one minute that capturing finish
8. Save the map of elements with using 'Save the map' button from file menu
9. Assign the specific colour to each element using colour button from toolbar menu

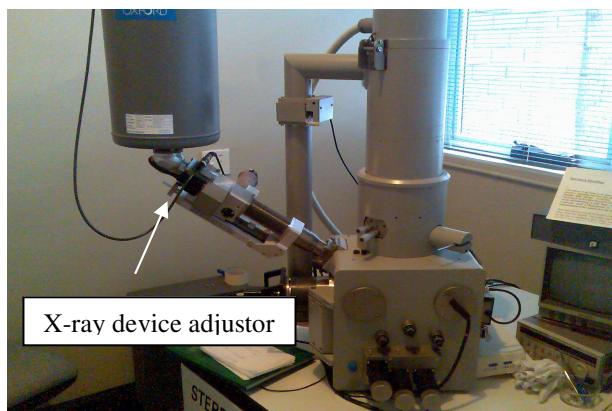


Figure 3-18: The X-ray device adjustor outside the SEM chamber.

3-8-2 TEM

3-8-2-1 Sample preparation

Transmission Electron Microscopy (TEM) and Scanning Transmission Electron Microscopy (STEM) in this work were carried out on a *Joel* 2011 JEM, 200KV system using a LaB₆ filament. The Chemical analysis was performed using Energy Dispersive Spectrometry (EDS), with an ultra-thin window. Images are taken using digital cameras and *SIS* image analysis software.

In order to prepare samples for the TEM imaging the fume particles generated on the Aluminium foil should be collected on the TEM grid as follows:

1. Prepare 60 ml filtered Ethanol as below:
 - a. Fill a 100 ml vial and 20 ml beaker with tap water and soap and put it in the ultrasonic (*UNISONIQUES, FX12F, 150 Hz*) bath for two minutes. Figure 3-19 shows the vial and beaker agitating in ultrasonic bath.
 - b. Wash the beaker and vial with adequate running tap water
 - c. Wash the beaker and vial it with Ethanol and let them dry
 - d. Fill the 5ml syringe with un-filtered Ethanol
 - e. Screw the 0.22 micrometer hydrophobic PVDF filter (*Millipore Millex-GV*) to the end of syringe. Figure 3-20 shows and filter locked at the end of the syringe.
 - f. Pour the Ethanol out of the syringe with filter in to the clean vial and repeat the procedure (d) and (e) to fill the vial
2. Fill one quarter of beaker with filtered Ethanol applying a new syringe
3. Place the beaker in the ultrasonic bath, while the bath is running
4. Wash the tweezers and scissors with Ethanol and let them dry
5. Cut the Aluminium foil around the place with the highest fume concentration with the scissors. Try not to touch the Aluminium foil with hand and use the tweezers. Figure 3-21 shows the cut Aluminium foil held with tweezers.
6. Hold the cut Aluminium foil with tweezers in the Ethanol agitating in the ultrasonic bath until all the fumes are suspended in the Ethanol
7. Place 5 sheets of A4 paper on the table and wash the top one in the middle with filtered Ethanol and let it dry
8. Place the holey Carbon-coated Cu grid on the washed paper with tweezers
9. Use the syringe to suck a millilitre of fume particulate suspended in Ethanol and drop it on the grid, normally three drops were enough
10. Put watch glass over the grid and leave to dry for about one hour. Figure 3-22 shows the grid on the washed paper covered by the watch glass while they are left for drying.
11. Pick the grid up with tweezers and put it inside the grid box and keep the reference of the compartment
12. Store the grid box in desiccator



Figure 3-19: The vial and beaker being cleaned in the ultrasonic bath.



Figure 3-20: The 5ml syringe and 0.22 micrometers PVDF Filter.

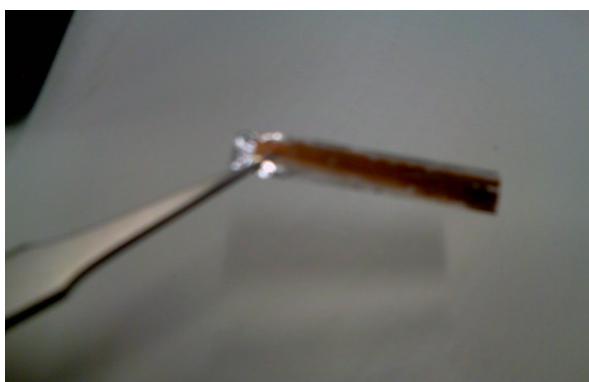


Figure 3-21: The cut Aluminium foil kept with tweezers before inserting into a beaker agitating in ultrasonic bath to wash the fumes into the filtered Ethanol.

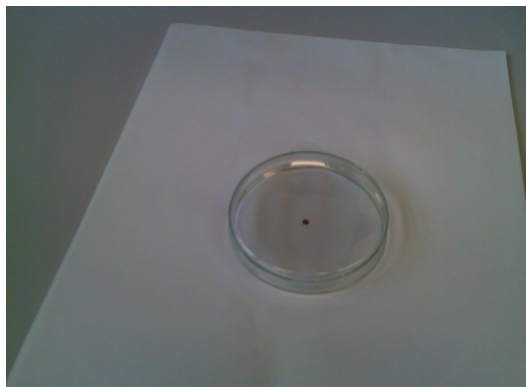


Figure 3-22: The holey Carbon-coated Cu grid on the washed paper, covered by the watch glass, while they are left to dry.

3-8-2-2 TEM Imaging

The effective time for implementing the TEM analysis on stored samples is less than 7 days. It is preferred to examine the specimen as soon as possible.

In order to run the TEM microscope the standard operating procedures must be followed. The pertinent points of the procedure are listed below:

1. Carefully pick one grid out of the grid box with fine tipped tweezers, only gripping the outer edge of the grid to prevent damage and fix it on the single-tilt TEM grid holder. Figure 3-23 shows the single-tilt TEM grid holder before installed inside the TEM Vacuum chamber.
2. Insert the grid holder to the initial position and allow ten minutes for the vacuum pump to pump down the chamber, before inserting specimen holder into final position
3. Turn the beam on at the standard accelerating Voltage of 180KV
4. Decrease the accelerating voltage to the 100KV, the beam current should be 56 microampere, with the operating bias set at 3:3
5. Align the beam and set eccentric height
6. For magnifications >100Kx the bottom digital camera (KEEN View) was used rather than the top digital camera (Mega view) to improve contrast and sharpness of image
7. Overlay the images with scale bar using the Option/Image/ Overlay with scale bar option
8. Save the images as Windows bitmap file (*.bmp) for following analyses



Figure 3-23: The specimen was placed in the single-tilt TEM grid holder.

3-8-2-3 EDS and STEM analyses

In order to implement the EDS analysis in bright field TEM mode, the beam needs to be focused on a single particle. In the case of particles $<20\text{nm}$ the beam is too wide and the EDS system can pick-up counts from surrounding or overlapping particles. In order to increase the reliability of the EDS results the Scanning Transmission Electron Microscopy (STEM) mode was implemented. Through the STEM technique, associated software allows automatic EDS analysis of selected particles, where a fine beam size of 9nm is produced. This fine beam-size enables the accurate chemical composition of small particles but care must be taken to select particles that are not overlapped. Figure 3-24 shows the TEM and STEM unit.

The procedure of the STEM is as follow:

1. Insert the STEM unit then push the 'wobbling' button twice to turn the STEM system on
2. Adjust the focus and contrast and take special care to ensure good alignment of 'voltage centre' and eccentric height
3. Capture the Image using the analysis station software and by pressing the image button on the toolbar
4. Choose the Sequential acquisition on the tool bar
5. Mark the particles on the image with pointer. The reference numbers appear next to the particles
6. Choose the start button, the STEM software automatically generates the EDS spectrum for each reference point
7. Save a copy of image and spectrum as (*.Jpg) format

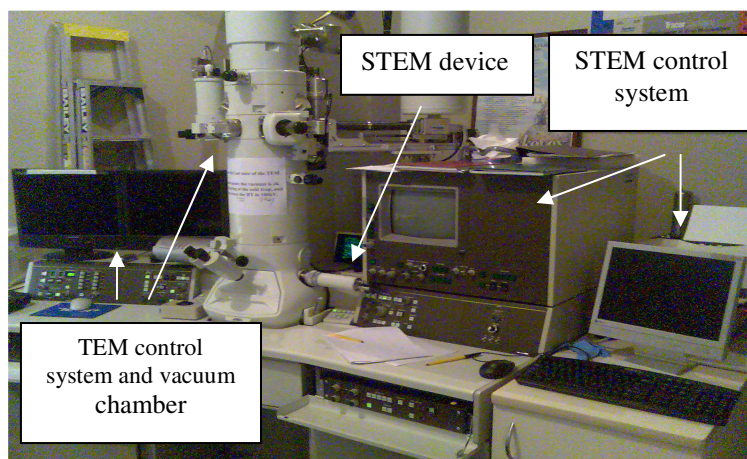


Figure 3-24: The *Joel 2011* TEM microscope and attached STEM control system.

3-8-2-4 Particle Size Analysis

To survey and analyse the fume particle size range, *Scion Image* software, downloadable from Internet, was applied. The *Microsoft Excel* template developed by Dr. Zoran Sterjovski (a researcher in University of Wollongong) was employed to interpret results.

To analyse the particles size and generate comparative charts the following procedure was developed:

1. Open Scion Image software
2. Choose File/ open and open a TEM Image with bitmap windows format
3. Choose the Analyse/ option and mark Perimeter/Length and Auto wand measurements
4. Draw three lines near the scale bar at exactly the same size
5. Select the Analyse/ show result
6. Choose wand from toolbar and select one of the drawn line
7. Choose Analyse/Set Scale and select nanometre as the scale and the length of the scale bar as 'known distance'
8. Choose the wand tools and select the two other lines. If the lengths of them shown in the result box are the same as the scale bar length on the Image, software is calibrated.
9. Draw a line exactly across each particle and for the faceted particles choose the biggest diameter
10. Choose Option/Threshold and set the LUT contrast on to the lowest part so only the lines are visible on the image
11. Choose Analyse/ Analyse particle
12. Choose Edit/ Copy measurements
13. Paste the results in the Microsoft Excel template

This template automatically generates the graphs of Normalised frequency and Cumulative frequency versus Particle diameter range from the input data.

CHAPTER FOUR

EXPERIMENTAL RESULTS

4-1 LASER chamber characteristics

In terms of considering the chamber measurement, the sample position adjustment can be quantified by LASER focal length. Table 4-1 shows the LASER focal length relation with sample position adjustment.

Results of spot size produced by different Focal lengths are shown in Table 4-2. The LASER Power for this experiment was 500W and time period of strike was 15sec. In order to examine the repeatability of experiment, in some cases the test has been repeated more than 5 times. The results are shown in figure 4-1 which shows the graph of LASER focal length versus the related average spot size.

The spot size diameter was also examined under different conditions (LASER Power: 300W and time period of strike: 15sec). These results are shown in table 4-3. The graph formed by the average spot sizes and related LASER focal length is shown in figure 4-2.

Both results of minimum spot sizes confirm that 200mm LASER focal length is produced with 290mm sample position adjustment.

Table 4-1: The LASER focal length relation with sample position adjustment.

Sample position adjustment(mm)	Related LASER focal length(mm)
280	210
282	208
284	206
285	205
286	204
290	200
294	196
295	195
300	190
310	180
320	170

Table 4-2: The spot size produced by different Focal length in 500W LASER power and 15 sec time of the strike.

Focal length (mm)	Spot size(mm)	Average	Divergence
210	6,6,6.2	6.06	0.01
208	5,5,6	5.33	0.08
206	5,5,4.8	4.93	0.01
205	5.5,5.4,5.5	5.46	0.08
204	5.5,5.6,5.3	5.46	0.02
200	4.5,4.5,4.3,4.5,4.5	4.46	0.01
196	5.5,5.4,5.5	5.46	0.08
195	6,5.8,5.8,6	5.9	0.01
190	6,6,6.2	6.06	0.01
180	6.5,6.8,6.5	6.6	0.02
170	9.7,7.7,2	7.06	0.01

Table 4-3: The spot size produced by different Focal length in 300W LASER power and 15 sec time of the strike.

Focal length)	Spot size diameter (mm)	Average	Divergence
206	4,4,4.2	4.06	0.02
204	4,4,3.8	3.93	0.02
200	4,3.8,3.8,3.8,3.8	3.84	0.02
196	4,4,4.2,4.2	4.1	0.02
192	4.5,4.5,4.5	4.5	0.00

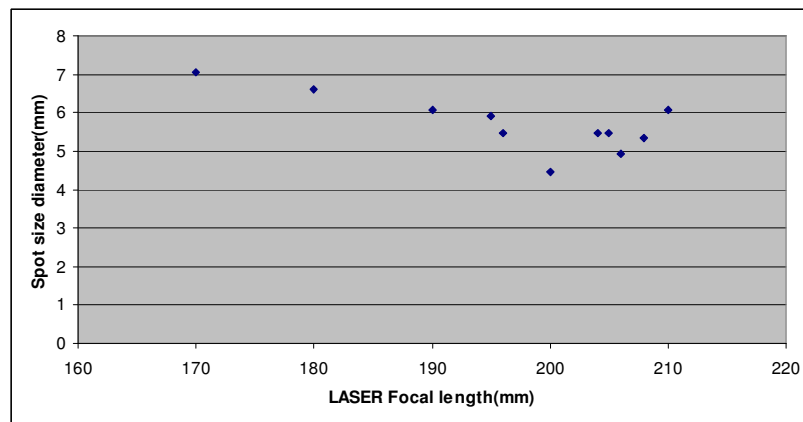


Figure 4-1: The graph of LASER Focal length versus the related average spot size produced in 500W LASER power and 15 sec time of strike.

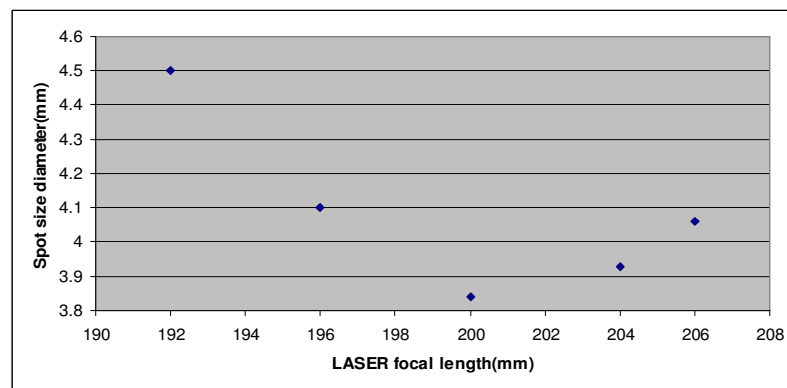


Figure 4-2: The graph of average spot size versus the related LASER focal length produced in 300W LASER power and 15 sec time of strike.

4-2 weighing experiments

To establish the standard deviation of the measure sample weight, a folded Aluminium foil (pattern shown in figure 3-10) weighed 10 times. The recorded results produced the standard deviation of 0.00154 gr. The results are shown in table 4-4.

In order to survey the repeatability, the weighing experiments were repeated five times. The condition of ablation for this experiment is: 300W LASER Power, 200mm LASER Focal length, 15 sec time of strike and Air atmosphere. Table 4-5 shows the result of this experiment.

The summary of generated fume weight in different LASER focal Length, LASER power, and atmosphere are shown in table 4-6. Figure 4-3 shows these results as a graph.

Keeping the time of strike constant on 20sec and varying the ablation condition, produces results shown in table 4-7. The results confirm 200mm LASER focal length generates the highest amount of fume in each atmosphere. Comparing the atmospheres together, the Air generates the highest amount of fume while CO₂, Argoshield52 and Stainshield 66 ranked after in order.

Table 4-4: The weighing results of folded Aluminium foil in order to set up the standard deviation of the Scales.

Times of weighing	i	ii	iii	iv	v	vi	vii	viii	ix	x
Weight	0.40489	0.40989	0.40988	0.40991	0.40992	0.40991	0.40987	0.4099	0.40991	0.40986

STDEV	0.00150 gr
Average	0.409394 gr

Table 4-5: The results of repeatability survey of weighing experiments. The condition of ablation is 300W LASER Power, 200mm LASER Focal length, 15 sec time of strike and Air atmosphere.

Trial	1	2	3	4	5
Fume generated weight	0.41270	0.41350	0.41420	0.41375	0.41390

STDEV	0.00051 gr
Average	0.413592 gr

Table 4-6: The summary of generated fume weights under different ablation conditions. The colours corresponding to different atmosphere described in table key.

	Focal length(mm)				Time of striking
		210	200	190	
LASER power (W)	100	0.39802*	0.40130	0.39982	15 Sec
	300	0.41090	0.41350	0.41210	
	500	0.42156	0.42380	0.42270	
	300	0.41086	0.41330	0.41202	30 Sec
	500	0.42295	0.42430	0.42328	
	300	0.41051	0.41279	0.41198	30Sec
	500	0.41563	0.41958	0.41712	
	300	0.40827	0.41152	0.41128	30 Sec
	500	0.41173	0.41372	0.41259	

Atmospheres:

	Air
	CO ₂ (gas code:081, size: G)
	Argoshield 52 (gas code: 070, size G)
	Stainshield 66 (gas code:093, size G)

*Generated fume weight (gr), the standard deviation ± 0.0015 gr should be considered. For example: the weight related to 0.39802 in table refers to $M=0.39802 \pm 0.0015$ gr.

Table 4-7: The generated fume weight with constant time of strike and LASER power but different LASER Focal length and atmosphere. The table key describe the different colours corresponding to different atmospheres.

	Focal Length (mm)				Time of striking
		210	200	190	
LASER power (W)	500	0.43096*	0.4358	0.43272	20sec
	500	0.35169	0.35632	0.35387	20sec
	500	0.30893	0.32179	0.32087	20sec
	500	0.27157	0.27564	0.27383	20sec

Atmospheres:

	Air
	CO ₂ (gas code:081, size: G)
	Argoshield 52 (Gas code: 070, size: G)
	Stainshield 66 (gas code:093, size: G)

*Generated fume weight (gr), the standard deviation ± 0.0015 gr should be considered. For example the weight related to 0.39802 in table refers to $M=0.43096 \pm 0.0015$ gr.

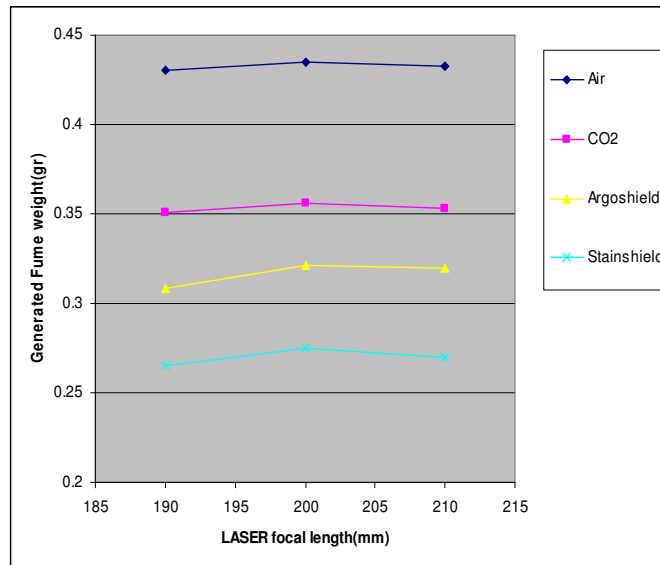


Figure 4-3: The comparative graph of generated fume weight in constant time of strike and LASER power but different LASER focal length, and Atmospheres. The table key describes the different colours corresponding to different atmospheres.

4-3 SEM

4-3-1 Images

Figures 4-4 and 4-5 show the SEM images of fume particulates and their morphology. It can be observed that most of the fume particles are in the range of sizes less than micrometer. While in figure 4-4 the minimum particles size which can be observed is 10 nm, resolving the fine fume particles with the SEM is quite hard to achieve. Figure 4-5 shows a particle bigger than 2 micrometers which was rarely observed in this work.

The micrometer-scale agglomeration pattern of the fume can only be surveyed with the SEM analysis. It has been observed that fumes in micrometer scale tend to agglomerate in patterns shown in figures 4-6 and 4-7 which are not affected by the different atmospheres.

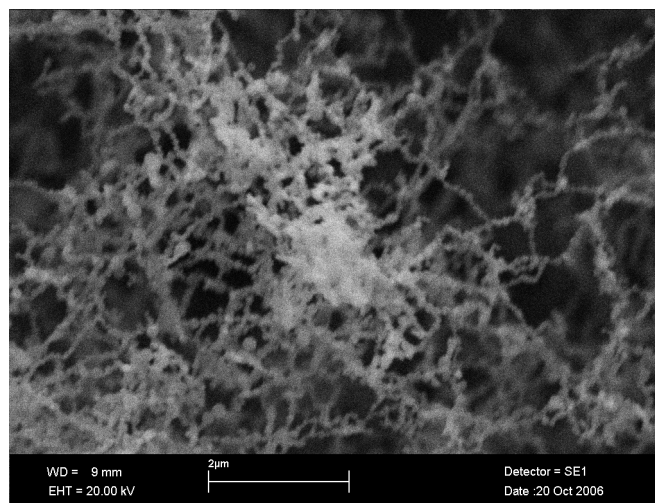


Figure 4-4: The SEM image of fume particulates and their morphology generated in Air, 300W LASER power and 200mm LASER focal length. Bar represents 2 micrometers.

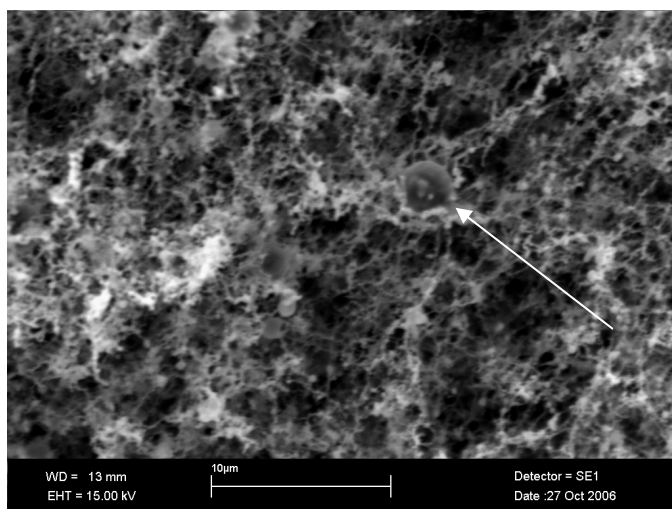


Figure 4-5: The SEM image of fume particles generated in Air, 300W LASER power and 210mm LASER focal length. Image shows a particle bigger than 2 micrometers which was rarely observed in this work. Bar represents 10 micrometers.

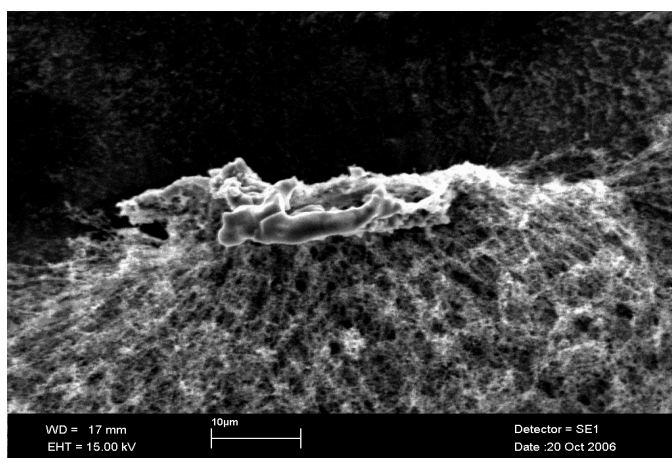


Figure 4-6: The SEM image of agglomeration pattern of fume particles generated in Air, 100W LASER power and 200mm LASER focal length. Bar represents micrometers.

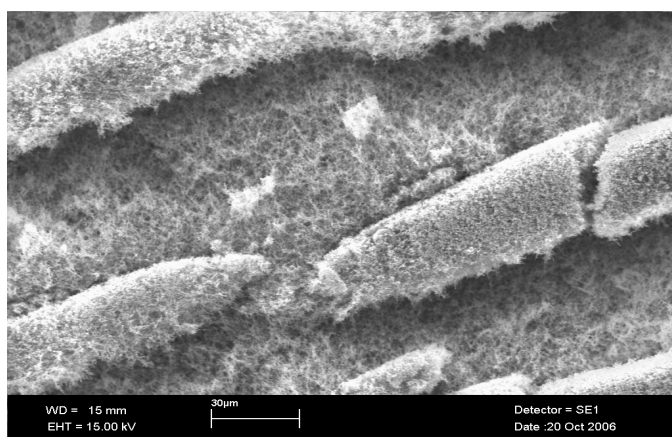


Figure 4-7: The SEM image of agglomeration pattern of fume particles generated in Air, 300W LASER power and 200mm LASER focal length. Bar represents 30 micrometers.

4-3-2 EDS and Map of elements

The EDS spectrums of all samples confirm the existence of Al (mainly from Aluminium foil), Fe, Mn, and Si.

The Map of elements analysis shows the ferrous compounds tend to be agglomerated together. This trend scarcely can be observed for Silicon and Manganese compounds.

Figure 4-8 shows the EDS spectrum of fume generated in 500W LASER power, 200mm LASER focal length and *Stainshield 66* atmosphere. Figures 4-9-a to 4-9-d show maps of elements of agglomerated fume particles which are captured through the SEM Imaging.

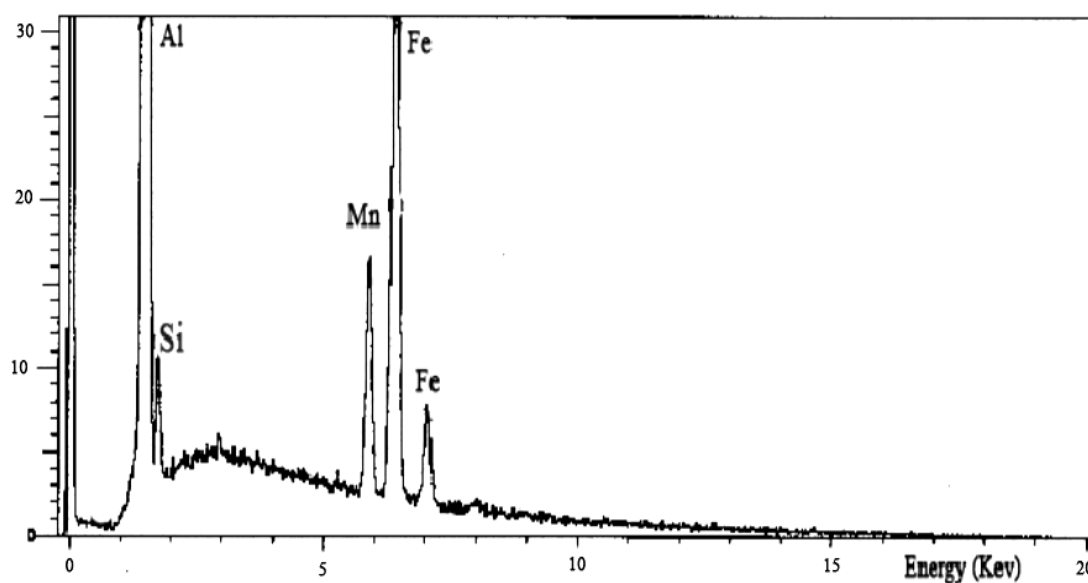
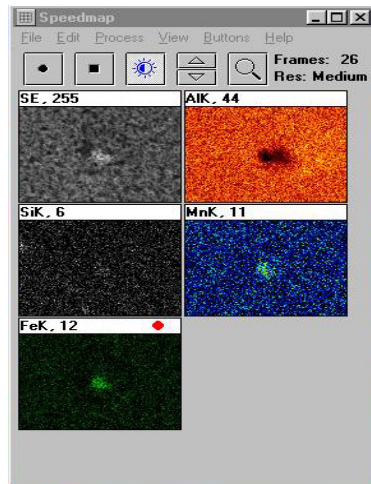
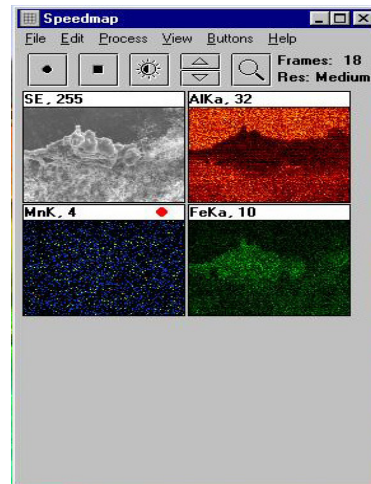


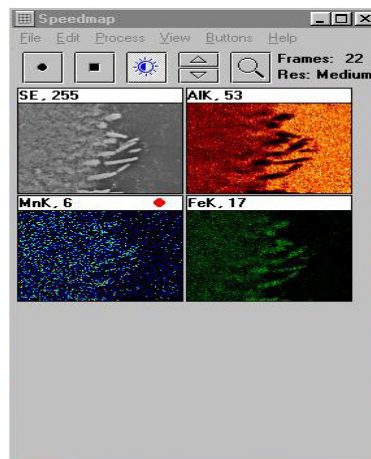
Figure 4-8: The EDS spectrum of fume generated in 500W LASER power, 200mm LASER focal length and *Stainshield 66* atmosphere.



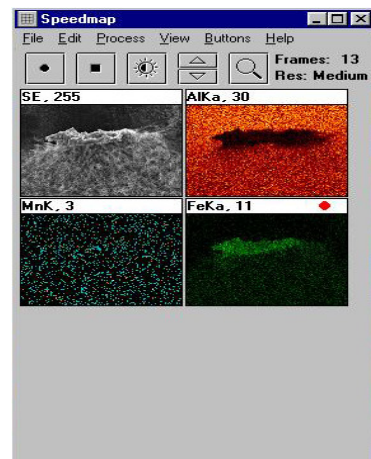
4-9-a



4-9-b



4-9-c



4-9-d

Figure 4-9: The maps of elements which are captured by the EDS method through the SEM Imaging;

- a) Generated in 300W LASER Power, 210mm LASER focal length and *Stainshield 66* atmosphere
- b) Generated in 300W LASER Power, 200mm LASER focal length and CO₂ atmosphere
- c) Generated in 500W LASER Power, 190mm LASER focal length and Argoshield atmosphere
- d) Generated in 500W LASER Power, 200mm LASER focal length and Air atmosphere

4-4 TEM

Table 4-8 shows the sample reference chart for the TEM and STEM analyses. These samples are generated at 300W LASER power, 200 mm LASER focal length and 20 sec time of strike.

Table 4-8: The sample reference table for the TEM and STEM analyses. The ablation condition is: 300W LASER power, 200 mm LASER focal length and 20 sec time of strike.

Atmosphere	Reference Number
Air	1
Argoshield 52	2
CO ₂	3
Stainshield 66	4

4-4-1 Images

The nanometre-scale morphology of fume particles can be investigated with the TEM analysis. Figure 4-10, representatively show the fume particles variation in different atmospheres while all the other ablation conditions (500W LASER power and 200mm LASER focal length) has been kept constant for comparison. These Images are used for particle size analysis using *Scion Images* software.

The fume particles observed in this work are mainly ‘faceted’, although in low magnification they seem to be ‘circular’. Figure 4-11 shows ‘faceted fume” In *Argoshield 52* atmosphere. Figure 4-12 shows the round and faceted fume agglomeration in *Argoshield52 atmosphere*. Figure 4-13 shows the agglomeration of round fume particles in Air.

Furthermore, it is observed that fume particles in the range of similar sizes tend to agglomerate in string like pattern (figure 4-14) but when the group of different sizes of particles are grouped together they vary in the pattern of agglomeration and population. Figure 4-15 shows the particles with different size agglomerates in ‘circular group’. Figure 4-16 shows the low magnification image of the fume particles shows that the group population varies between 3 to 400 particles.

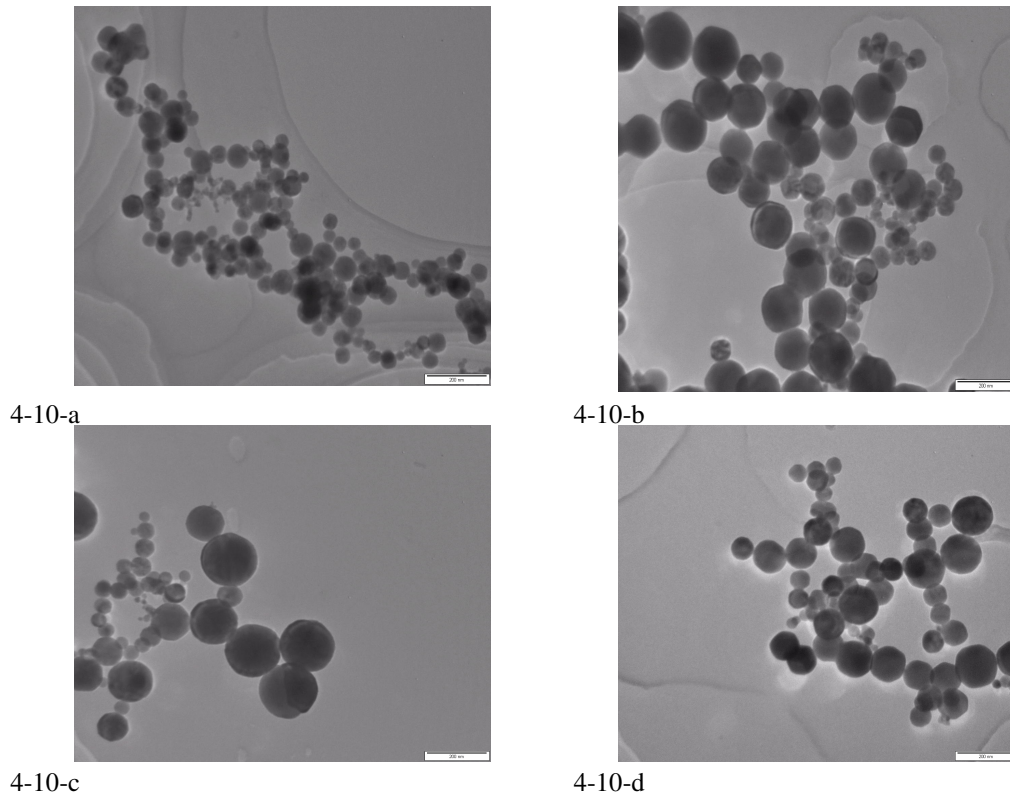


Figure 4-10: The bright field images of fume particles generated in 500W LASER power and 200mm LASER focal length. Bars represent 200nm.

Representative fume particles generated in:

- a) Stainshield 66.
- b) Argoshield 52
- c) Air
- d) CO₂

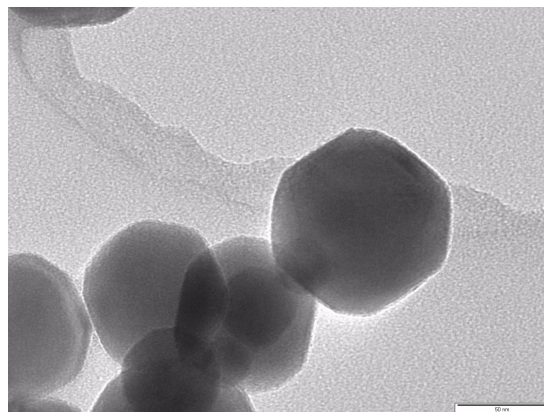


Figure 4-11: The KEEN View (Bottom camera) bright field image of fume particles generated in 500W LASER power, 200mm LASER focal length and in the Argoshield 52 atmosphere. Image shows the faceted fume particles. Bar represents 50nm.

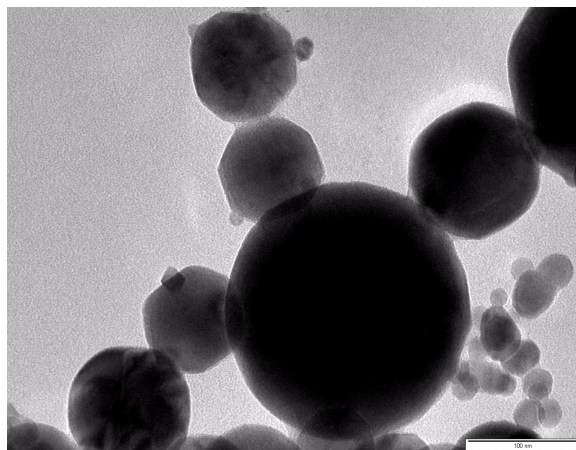


Figure 4-12: The KEEN View (Bottom camera) bright field image of fume particles generated in 500W LASER power, 200mm LASER focal length and in the Argoshield 52 atmosphere. Image shows the 'round' and 'faceted' fume particles agglomeration. Bar represents 100nm.

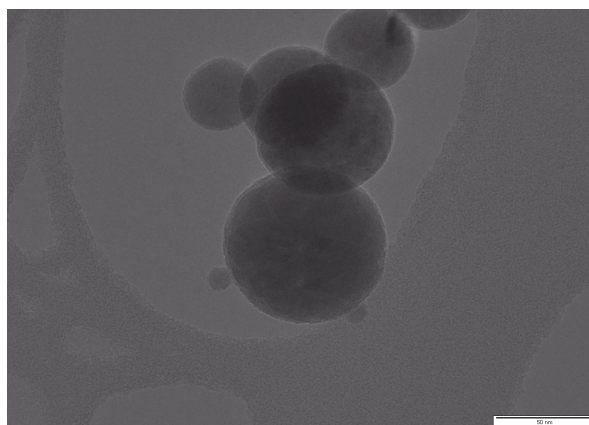


Figure 4-13: The KEEN View (Bottom camera) bright field image of fume particles generated in 500W LASER power, 200mm LASER focal length and in the air. Image shows the 'round' fume particles. Bar represents 50nm.

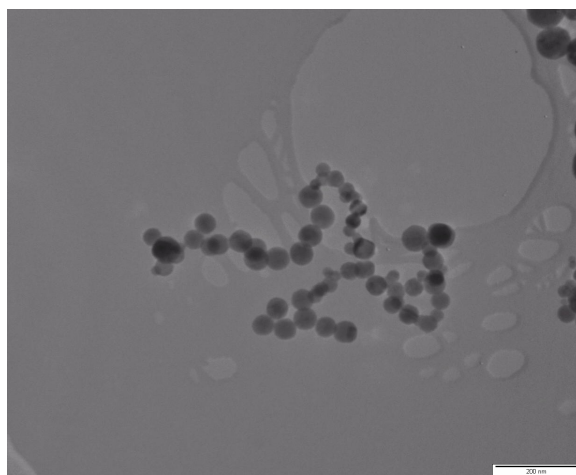


Figure 4-14: The bright field image of fume particles generated in 500W LASER power, 200mm LASER focal length and in the Air. Image shows 'string like' pattern of fume particles agglomeration. Bar represents 200nm.

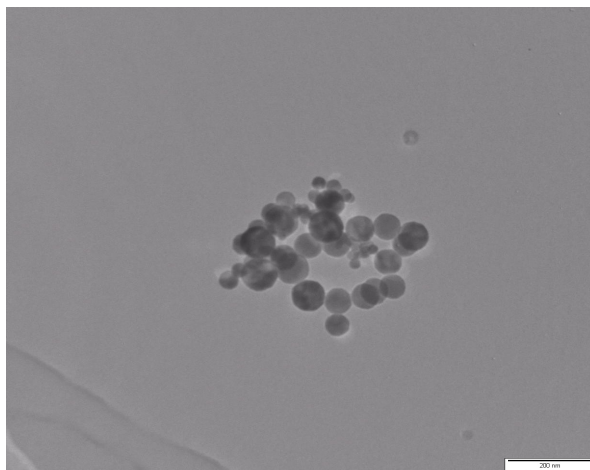


Figure 4-15: The bright field image of fume particles generated in 500W LASER power, 200mm LASER focal length and in the Air. Image shows fume particles with different sizes agglomerated in 'circular group'. Bar represents 200nm.

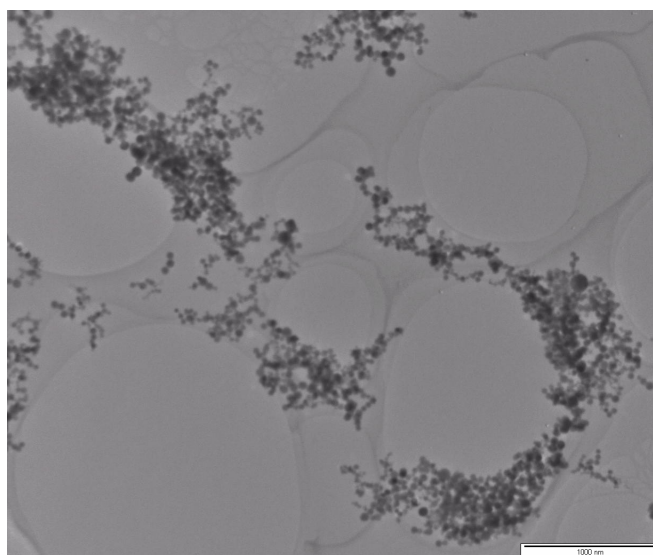
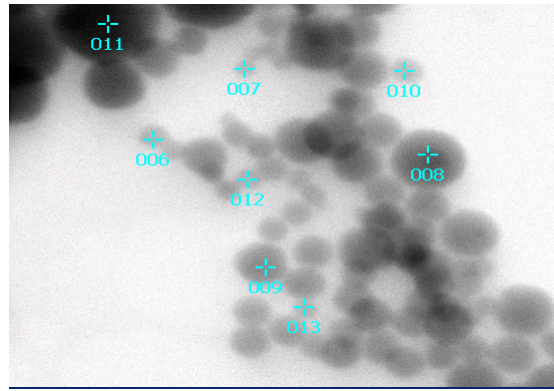


Figure 4-16: The low magnification bright field image of fume particles generated in 500W LASER power, 200mm LASER focal length and in the Stainshield 66 atmosphere. Image shows the groups of fume particles population vary between 3 to 400 particles. Bar represents 1000nm.

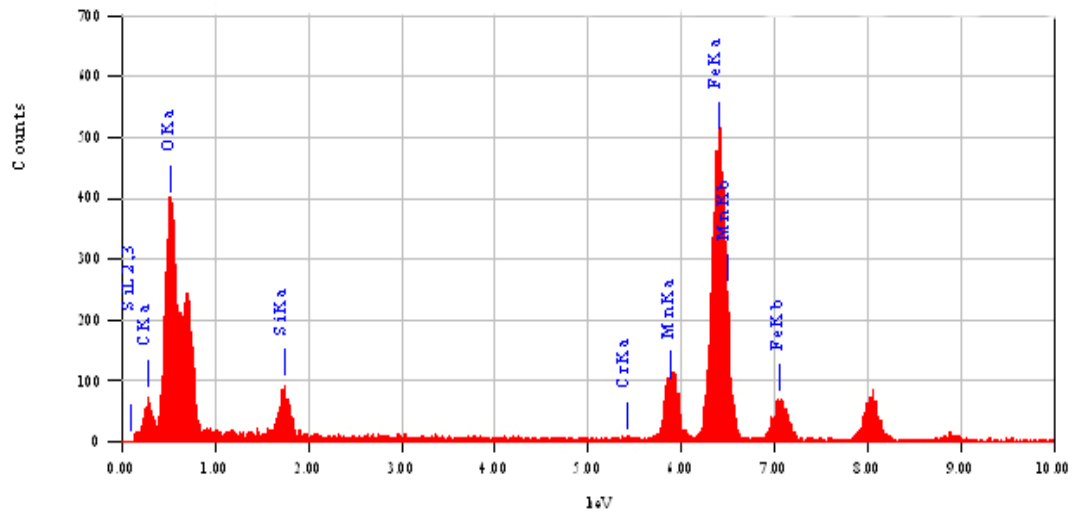
4-4-2 EDS and map of elements

The EDS analysis of fume particles applying the STEM techniques confirms the existence of Fe, Mn, Si and Oxygen in fume chemical compound. Although the bigger fume particles generate the bigger peaks in Spectrum, The recognised elements in all range of the fume particles sizes are the same. Figure 4-17 shows the EDS results of particles where one big and one small particle spectrum are chosen, representatively for comparison.

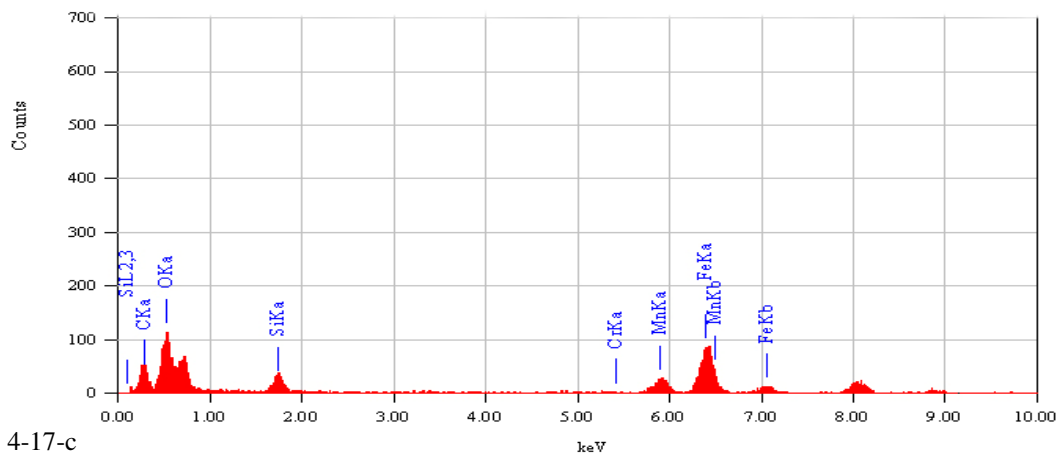
The EDS analysis through the SEM experiments does not show the existence of Oxygen. For better survey map of elements with the STEM techniques was carried out. Figure 4-18 shows the map of elements captured through the STEM technique. It shows the dispersion of elements and confirms the existence of Oxygen.



4-17-a



4-17-b



4-17-c

Figure 4-17: The EDS spectrums captured with the STEM techniques through the TEM analysis.

- Shows the TEM Image of fume generated in *Argoshield 52* atmosphere, 500W LASER power and 200mm LASER focal length. The Image is captured at 300 Kx magnifications.
- Shows the spectrum of particle referenced as No. 11 on Image(a)
- Shows the spectrum of particle referenced as No. 6 on Image(a)

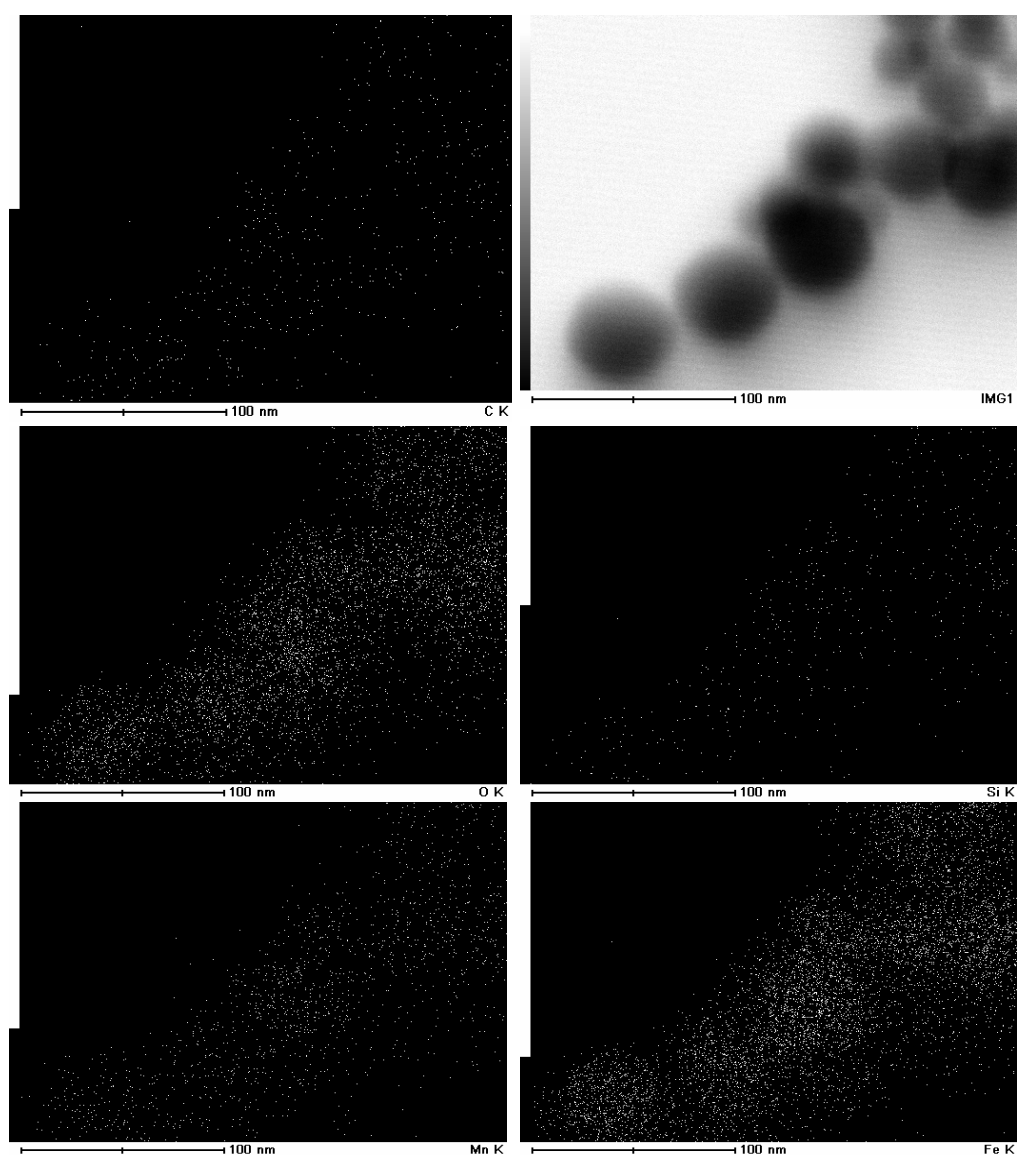


Figure 4-18: The STEM Map of elements of fume particles generated in 500W LASER power, 200mm LASER focal length and in Argoshield52 atmosphere. Bars represent 100nm.

4-4-3 Particle Size Analysis

The particle size analysis carried out by Scion Image software produced the comparative graph shown in figures 4-19 and 4-20. Figure 4-19 shows the comparative histogram of Normalised frequency versus fume particle diameter (nm) for different atmospheres. Figure 4-20 shows the comparative cumulative histogram of fume particle diameter (nm) for different atmospheres.

In order to examine the reproducibility of experiments the particle size analysis has been carried out three times for sample No.1 (table 4-8). The results of these three trials are shown in diagram of figure 4-21. The

results shown in the diagram are for ablation condition No.1 (table 4-8). Also, the results of some fume particle size analyses repeated for two times are shown in table 4-9.

For better investigation all the other analyses for different conditions have been carried out two times. The result of these analyses is shown in table 4-9.

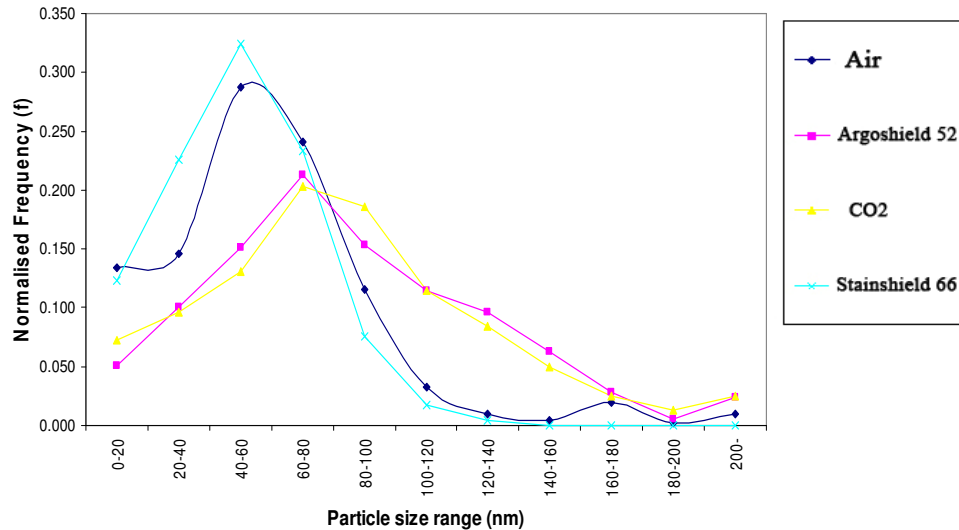


Figure 4-19: The Histogram of Normalised frequency versus fume particle diameter (nm). The ablation condition is: 300W LASER power, 200 mm Laser focal length and 20sec time of strike.

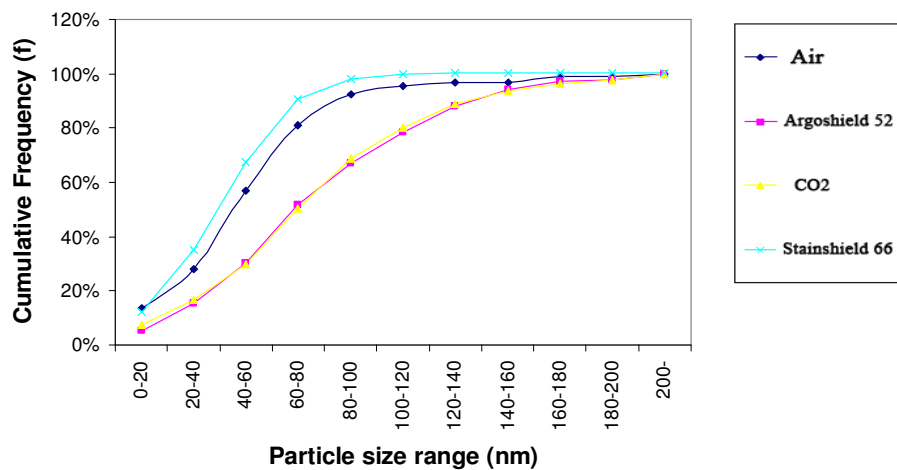


Figure 4-20: The comparative cumulative histogram of fume particle diameter (nm) for different atmospheres.

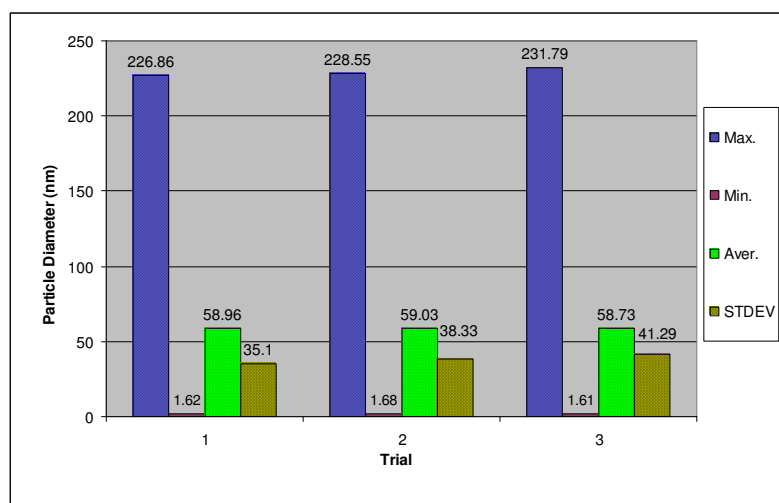


Figure 4-21: The comparative diagram of Maximum, Minimum, Average and standard deviation of three different trials with *Scion Image software*. The results of trials are related to ablation condition No.1 (table 4-8).

Table 4-9: The result of fume particle size analysis repeated for two times.

Sample Reference Number	Trial	Max	Min	Aver
2*	I	295.09	1.42	88.03299
	II	302.24	2.33	85.63179
3	I	363.23	1.62	76.86575
	II	352.76	1.62	74.38167
4	I	128.24	1.62	47.3668
	II	136.54	2.42	49.76283

* The number coordinates with ablation condition shown in table 4-8.

CHAPTER FIVE

DISCUSSION

Although fume exposure limits are published by several organisations (table 2-11) [4] and controls measures suggested in such as standard ANSI Z49.1, “safety in welding and cutting” [3], try to minimise the impact of fume particles on welders health, still long-term even acute consequences of fume exposures are reported [1,2] . Considering the factors which can affect welder health, fume particle size is one of the key factors [38].

Beside the substantial work which has been done on investigating the fume particle sizes, discrepancies in literature can be observed. The reported fume particles sizes are often larger than those observed in this work. The fume particles in this work are mainly less than 0.1 micrometer, ‘ultra-fine particle’, which according to some reports can directly affect human health [38].

5-1 Chamber characteristics

When the LASER spot was focussed on the surface of the sample the spot size was minimized in both figures 4-1 and 4-2 and the highest amount fume was generated.

The repeatability of generated spot size shows the divergence to be less than 0.02mm. By comparing figures 4-1 and 4-2, it is also observed that reproducibility of experiment and trend of generated spot size are independent of LASER power.

5-2 Weighing experiments

The standard deviation of the sample weight was examined after finding the standard size and method of folding the Aluminium foil (figure3-10). A standard deviation is: 0.00154 gr (table 4-4) was established. This standard deviation should be considered in subsequent weighing results as (± 0.00154 gr). Since the minimum difference in weight of generated fume is: 0.004 gr, the standard deviation is negligible.

The reproducibility of weighing experiments was examined before proceeding to carry out the weighing experiments for different atmospheres. Table 4-5 shows the results of five repetitions of the weighing experiments for a specific ablation condition (300W LASER Power, 200mm LASER focal length, 15 sec time of strike and Air atmosphere). The results of standard deviation show the negligible variation which confirms the repeatability of weighing experiments.

The results of weighting experiment show that the Air atmosphere generates the highest amount of fume while CO_2 , *Argoshield 52* and *Stainshield 66* produced successively lower amounts. It is possible that the existence of H_2 in *Stainshield 66* decreases its oxidation potential. Also, pure CO_2 shows a higher oxidation potential than mixture of Argon and hydrogen. Moreover, Adding CO_2 and O_2 to Ar increases the FFR (Fume Formation Rate) in GMAW process [41]. This effect is shown in table 2-12 and figure 2-2. The results of weighing experiment applying LASER ablation in current work also shows the higher amount of

generated fume in *Argosheild 52* comparing to *Stainshield 66*. The higher amount of CO_2 in *Argosheild 52* as described in literature is responsible for generating higher amount of fume in comparison with *Stainshield 66*.

5-3 Fume particles size

Using the different sampling methods described in AS 3853 2-1991 [33], Jenkins & Eager suggest that the size range of fume particles varies with analytical methods [35]. They mention the fume particles in the range of 0.5-50 micrometer can be analysed with the SEM while the TEM can survey the fume particles with 0.001-1 micrometer [35].

Fume particles are normally in the range of 0-2 micrometers in diameter while they can agglomerate up to 10 micrometers [1]. The fume particles less than 0.1 micrometer in diameter are considered as 'Ultra fine' particles [38]. In the current work the minimum particle size observed with the SEM is 0.1 (figure 4-4) although is hard to resolve particles less than 0.60 micrometers. The maximum observed particle size found by the SEM imaging was 2.8 micrometer (figure 4-5). The range of the particles observed with the TEM analysis was 0.1-0.358 micrometers while the TEM imaging shows the ability to resolve particles of 0.05 micrometer diameter.

The Scion Image software was used to survey the particles size in different atmospheres. Firstly in order to assess the reproducibility of analysis, three trials for a specified ablation condition were carried out. Figure 4-21 shows the $\pm 2.7233\text{nm}$ deviation between the maximums of particle size as well as $\pm 0.17667\text{nm}$ for averages and $\pm 0.26667\text{nm}$ for minimum particles size which are negligible. Moreover, $\pm 3.14\text{nm}$ aberration for the Standard deviations is acceptable. As a result, it is considered that conducting the particle size analysis using the described sampling method results in reproducible data.

Changing the atmospheres does not dramatically change the minimum generated particle size and approximately 1.62nm is the size of smallest particle for all of the applied atmospheres.

Although the particles in the size range greater than micrometer were rarely observed through the SEM imaging (figure 4-5), the largest particle size with the TEM for CO_2 atmosphere is 357.99nm, for *Argosheild 52* is 298.66nm, for Air is 229.06nm and for *Stainshield 66* is 132.39nm.

Je Yu, et al. during the study of MMA of Stainless steel with the TEM analysis show the mean diameter of 0.1 micrometer for particles size with same pattern of cumulative frequency shown in figure 2-9 [37]. The average particle size observed for *Argosheild 52* is 86.83nm, for CO_2 is 75.62 nm, for Air is 58.90 nm, and for *Stainshield 66* is 48.56 nm. The observed average particles size are fairly smaller than what are previously reported in the literature.

Stainshield 66 tends to generate the fume particles in a range of less than 50nm. This tendency with *Air* is shifted to slightly larger particles (60 nm) and 70 nm is typical for *Argoshield 52*. Finally, 80nm is the highest frequency of generated fume particles for *CO₂* atmosphere.

5-4 Fume morphology

The micron scale morphology of fume could only be examined with the SEM, since the natural agglomeration of fume particles (figures 4-4, 4-5, 4-6 and 4-7) might be disturbed after they were washed out of the Aluminium foil. Although there is possibility that the TEM imaging shows a different pattern of agglomeration, the only potential method for nanometre-scale analysis of morphology is the TEM because investigating the nanometre-scale morphology of fume particles with the SEM is very hard to achieve.

The more frequent agglomeration pattern of fume particles, independent of applied atmosphere is as three dimensional networks of particles shown in figure 4-4. Decreasing the magnification and having observed the 30 micrometers scale of fume shows the large-scale agglomeration pattern of fume particles; figure 4-7. The map of elements (figure 4-9) shown by the EDS analysis confirms that the ferrous particles are the main compounds of this network of fumes while the other formative elements tend to disperse evenly.

According to literature the fume particles morphology is divided into three different categories as ‘individual’, ‘chain’ and ‘agglomerated particles’ [29]. The individual fume particles can be up to 400 nm in diameter while ‘chains’ can grow up to several micrometers and the agglomerated particles up to 500nm [29]. The ‘chains’ in this work grew up to 10 micrometer while the agglomerated group can be as large as several micrometers.

It has been observed that in ‘chain’ pattern, the fume particles are in the range of similar sizes (figure 4-14), but when the group of different sizes of particles group together they vary in the patterns of agglomeration and population. In one of the common recognized pattern of agglomeration, the particles with different sizes agglomerate in a ‘spherical’ group (figure 4-15). Figure 4-16, the low magnification image of the fume particles shows that the group population varies between 3 to 400 particles.

Mainly the particles during MMAW, GMAW, and TIG are reported as spherical particles [29].

The fume particles observed in this work are mainly ‘faceted’ (figure4-11). Although at low magnification they seem to be circular, increasing the resolution by using the bottom camera in the TEM shows the faceted particles. However, both circular (figure4-12) and ‘faceted’ fume are observed in all atmospheres.

5-5 Fume particles compounds

A chemical composition survey carried out with the X-ray, STEM and SPEC mainly identifies the presence of K, Fe, Cr, Mn, Ca, Si, Al, and Ca [29].

Using the EDS on the SEM illustrate the existence of Al, Fe, Mn and Si (figure 4-8). Similarly, these elements are observed to exist in all the other fume particles generated in different atmospheres and ablation conditions, despite the differences in the counted peaks. Owing to the use of Aluminium foil as foundation for fume, it may be concluded that the Al peak resulted from condensation from the foil. Since, the results of the EDS through the STEM technique (figure 4-17) do not show the existence of Al, it can be omitted from the list of fume formative elements.

Moreover, the EDS results through the STEM technique also show that the composition of the particle is not a variable of particle size. As shown in figure 4-17 the larger particle spectrum shows the same elements as the smaller particles.

5-6 Recommendations

The Investigating of the size distribution and morphology of fume are recommended while different welding electrodes are targeted by LASER and atmosphere is purged with shielding gases. For this purpose a technique should be established to generate fume only from electrode coating and not the metal core. A possible solution might be using the powder of electrode coating bounded with volatile resin.

CHAPTER SIX

CONCLUSIONS

- A technique for controlled generation of particulate by LASER ablation has been developed.
- The average fume particle size observed in all atmospheres was less than 0.1 micrometer.
- CO₂ generated the largest fume particles compared to Ar, while adding H₂ led to smaller particles size.
- The survey of the agglomerated fume particles morphology with the SEM is more reliable since the TEM sample preparation might disturb the agglomeration pattern.
- Fume particles agglomeration tended to grow three dimensionally while ferrous compound tended to make network and agglomerated together.
- The fume particles in the same size range tended to agglomerate in a 'chain' pattern which could grow up to 10 micrometers.
- The population of agglomerated particles with different sizes together varied between 3 and 400 particles. One of the most common patterns of these agglomerations was 'spherical' pattern.
- Fume particles were mainly 'faceted' independent of applied atmosphere.
- Fe, Mn, Si and O₂ were the elements observed in fume particles composition and the elements found in the fume particles did not vary in different atmospheres.

REFERENCES

- [1]. Slater, G.R., 2004, *Welding fume plume dispersion*, PhD thesis, University of Wollongong, viewed 20/03/20096, < <http://www.library.uow.edu.au/adt-NWU/public/adt-NWU20050307.120815/>>
- [2]. Sadek, A.H., Rauch, R. & Schulz, P.E., 2003, 'Parkinsonism due to Manganism in a Welder', *International Journal of Toxicology*, Volume 22, Number 5, Sep-Oct 2003, pp. 393- 401, Viewed 02/04/2006, (Available: Taylor & Francis, University of Wollongong Database).
- [3]. Ashby, H.S., 2002, *Welding fume in work place*, April, viewed 27/03/2006, <www.aiha.org/localsections/html/NTS/0602News1.pdf>
- [4]. Wallace, M.E., Fischbach, Th., Kovein, R.J., 1997, *In-Depth Survey Report: Control Technology Assessment for the Welding Operations*, Boilermaker's National Apprenticeship Training School Kansas City, Kansas, June 27, viewed 28/03/2006, <http://www.osha.gov/SLTC/weldingcuttingbrazing/report_boilermakers/boilermakers.html>
- [5]. Cohen, M.D., 'Pulmonary Immunotoxicology of Select Metals: Aluminium, Arsenic, Cadmium, Chromium, Copper, Manganese, Nickel, Vanadium, and Zinc', *Journal of Immunotoxicology*, 1:39-69, 2004, ISSN: 1547-691X print / 1547-6901 online, pp. 39-69, viewed 20/03/2006, (Available: Taylor & Francis, University of Wollongong Database).
- [6]. Toxicological Profile Information Sheet, 1999, *Toxicological Profile for Aluminium*, U.S. Department of Public Health and Human Services, Agency for Toxic Substances and Disease Registry, update; PB/99/166613, viewed 10/04/2006, < <http://www.atsdr.cdc.gov/toxprofiles/tp22.html>>
- [7]. Toxicological Profile Information Sheet, 2000, *Toxicological Profile for Arsenic*, U.S. Department of Public Health and Human Services, Agency for Toxic Substances and Disease Registry, update; PB/2000/108021, viewed 8/04/2006, < <http://www.atsdr.cdc.gov/toxpro2.html>>
- [8]. Toxicological Profile Information Sheet, 1999, *Toxicological Profile for Cadmium*, U.S. Department of Public Health and Human Services, Agency for Toxic Substances and Disease Registry, Update; PB/99/166621, viewed 11/04/2006, < <http://www.atsdr.cdc.gov/toxpro2.html>>
- [9]. Toxicological Profile Information Sheet, 2000, *Toxicological Profile for Chromium*, U.S. Department of Public Health and Human Services, Agency for Toxic Substances and Disease Registry Update; PB/2000/108022, viewed 8/04/2006, < <http://www.atsdr.cdc.gov/toxpro2.html>>
- [10]. Toxicological Profile Information Sheet, 2002, *Toxicological Profile for Copper*, U.S. Department of Public Health and Human Services, Agency for Toxic Substances and Disease Registry updates; PB 2004-10733, viewed 12/04/2006, < <http://www.atsdr.cdc.gov/toxpro2.html>>

- [11]. Toxicological Profile Information Sheet, 2000, *Toxicological Profile for Manganese*, U.S. Department of Public Health and Human Services, Agency for Toxic Substances and Disease Registry update; PB/2000/108025, viewed 10/04/2006, < <http://www.atsdr.cdc.gov/toxpro2.html>>
- [12]. Toxicological Profile Information Sheet, 2005, *Toxicological Profile for Nickel*, U.S. Department of Health and Human Services, Agency for Toxic Substances and Disease Registry, update; PB2006-100005, viewed 8/04/2006, < <http://www.atsdr.cdc.gov/toxpro2.html>>
- [13]. Toxicological Profile Information Sheet, 1992, *Toxicological Profile for Vanadium*, U.S. Department of Public Health and Human Services, Agency for Toxic Substances and Disease Registry, PB/93/110880/AS, viewed 11/04/2006, < <http://www.atsdr.cdc.gov/toxpro2.html>>
- [15]. Toxicological Profile Information Sheet, 2005, *Toxicological Profile for Zinc*, U.S. Department of Public Health and Human Services, Agency for Toxic Substances and Disease Registry, PB2006-100008, viewed 14/04/2006, < <http://www.atsdr.cdc.gov/toxpro2.html>>
- [16]. Antonini, J.M., 2003, 'Health effects of welding', *Critical Reviews in Toxicology*, Volume 33, Number 1, 2003, pp. 61-103, viewed 22/03/2006, (Available: Taylor & Francis, University of Wollongong Database).
- [17]. Balkissoon, R., 2006, 'A 26-Year-Old Welder with Severe Non-Reversible Obstructive Lung Disease', *Journal of Chronic Obstructive Pulmonary Disease*, Volume 3, Number 1, pp. 63-67, viewed 02/04/2006, (Available: Taylor & Francis, University of Wollongong Database).
- [18]. Borak, J., Cohen, H., Hethmon, Th.A., 2000, 'Copper Exposure and Metal Fume Fever: Lack of Evidence for a Causal Relationship', *AIHA Journal*, Volume 61, Number 6, pp. 832-836, viewed 28/03/2006, (Available: Taylor & Francis, University of Wollongong Database).
- [19]. Hotz, Ph., 2003, 'Cadmium, Lung and Prostate cancer: A systematic review of recent Epidemiological data', *Journal of Toxicology and Environmental Health part B*, Volume 6, Number 3, pp. 227-256, viewed 02/04/2006, (Available: Taylor & Francis, University of Wollongong Database).
- [20]. Mur, J.M., Teculescu, D., Pham, Q.T., Gaertner, M., Massin, N., Meyer-Bisch, C., Moulin, J.J., Diebold, F., Pierre, F., Meurou-Poncelet, B., et al., 1985, *Lung function and clinical findings in a cross-sectional study of arc welders, An epidemiological study*, Abstract, viewed 14/04/2006, <http://www.ncbi.nlm.nih.gov/entrez/query.fcgi?cmd=Retrieve&db=PubMed&listuids=_4077277&dopt=Abstract>
- [21]. Beckett, W.S., Pace, P.E., Sferlazza, S.J., Perlman, G.D., Chen, A.H., Xu, X.P., 1996, *Airway reactivity in welders: a controlled prospective cohort study*, Abstract, viewed 09/03/2006,

<http://www.ncbi.nlm.nih.gov/entrez/query.fcgi?cmd=Retrieve&db=PubMed&list_uids=8978514&dopt=Abstract>

- [22]. Sjogren, B. 2004, 'Flouride exposure and respiratory symptoms in welders', *International Journal of occupational and Environmental Health*, July-September, p. 310, viewed 17/03/2006, (Available: Proquest5000, University of Wollongong Database).
- [23]. Verma, D.K., 2000, ' Adjustment of Occupational Exposure Limits for Unusual Work Schedules', *AIHA Journal*, Volume 61, Number 3, pp. 367-374, viewed 21/03/2006, (Available: Taylor & Francis, University of Wollongong Database).
- [24]. Herbrt, Ch.G., Johnston, R.A.W., 2003, *Mass spectrometry basic*, CRC Press LLC, United States of America.
- [25]. Sylvester, P., (ed.), 2001, *Laser-ablation-ICPMS in the earth sciences principals and applications*, Volume 29, ST. John's, Newfoundland, Canada.
- [26]. Wikipedia, 2006, *List of the LASER types*, May, viewed 25/03/2006,
< http://en.wikipedia.org/wiki/List_of_laser_types>
- [27]. Miller, C.B., (n.d.), *LASER welding article*, viewed 12/03/2006,
< <http://www.uslasercorp.com/envoy/welding.html>>
- [28]. NUVONYX, 2000, *Benefits of direct diode Lasers for welding*, viewed 01/04/2005,
<<http://www.nuvonyx.com>>
- [29]. Standard Australia, 2003, *shielding gas for welding*, AS 4882-2003, pp. 1-10, viewed 10/03/2006,
(Available: Australian standards online via University of Wollongong Database).
- [30]. Kelly, A., 1996, *What is a CCD camera and how does it work?*, April, viewed 27/04/2006,
< <http://www.ghg.net/akelly/ccdbasic.htm>>
- [31]. EXview HAD CCD, (n.d.), *Improved Picture Quality and Increased Functionality Black-and-White CCD Camera System*, viewed 28/04/2006,
< <http://www.rfconcepts.co.uk/cxd2463r.pdf>>
- [32]. Standard Australia, 1991, *Fume from welding and allied processes Part 1: Guide to methods for the sampling and analysis of particulate matter*, AS 3853.1—1991, pp. 1-14, viewed 02/05/2006,
(Available: Australian standards online via University of Wollongong Database).

- [33]. Standard Australia, 1991, *Fume from welding and allied processes Part 2: Guide to methods for the sampling and analysis of gases*, AS 3853.2—1991, pp. 1-14, viewed 18/04/2006, (Available: Australian standards online via University of Wollongong Database).
- [34]. International Standard, *processes — Laboratory methods for sampling fume and gases generated by arc welding —Part 1: Determination of emission rate and Sampling for analysis particulate fume*, ISO 15011-1, pp. 1-19, viewed 20/04/2006, (Available: Australian standards online via University of Wollongong Database).
- [35]. Jenkins, N.T. & Eager, T.W., 2005, *Chemical Analysis of Welding Fume Particles*, June, viewed 22/04/2006, < <http://files.aws.org/wj/supplement/06-2005-JENKINS-s.pdf>>
- [36]. Antonini, J.M., Afshari, A.A., Stone, S., Chen, B., Schwegler-Berry, D., Fletcher, G.W., Goldsmith, W.T., Vandestouwe, K.H., McKinney, W., Castranova, V., Frazer, D.G., 2006, 'Design, Construction, and Characterization of a Novel Robotic Welding Fume Generator and Inhalation Exposure System for Laboratory Animals', *Journal of Occupational and Environmental Hygiene*, vol. 3, Number 4, April, viewed 09/03/2006, (Available: Taylor & Francis, University of Wollongong Database).
- [37]. Yu J., Kim, K.J., Chang, H.K., Song, K.S., Han, K.T., Han, J.H., Maeng, S.H., Chung, Y.H., Park, S.H., Chung, K.H., et al., 2000, 'Pattern of deposition of stainless steel welding fume particles inhaled into the respiratory systems of Sprague–Dawley rats exposed to a novel welding fume generating system', *Toxicology Letters*, Volume 116, July, pp. 103-111, viewed 25/003/2006, (Available: Science Direct, University of Wollongong Database).
- [38]. Augustin St., 2002, *The formation of ultra-fine particles during welding and allied processes*, July, viewed 20/03/2006, < http://www.nmbg.de/files/104/ultrafeine_partikel_eng.pdf>
- [39]. Jenkins, N., 1999, *Welding Fume Formation*, viewed 02/09/2006, <<http://neiljenkins.net/Fume/fumetheoryreview.pdf>>
- [40]. Mendez, P.F., Jenkins, N.T., Eager, T.W., 2000, *Effect of electrode droplet size on evaporation and fume generation in GMAW*, viewed 10/09/2006, <<http://eagar.mit.edu/EagarPapers/Eagar181.pdf>>
- [41]. Pires, I., Quintino, L., Miranda, R.M., 2006, 'Analysis of the influence of shielding gas mixture on the gas metal arc welding metal transfer modes and fume formation rate', *Material and Design*, viewed 27/ 08/2006, (Available: science direct, University of Wollongong Database).

APPENDIX

The two following pages show the AutoCAD initial drawings of LASER ablation chamber described in section 3-1.